AMERICAN SOCIETY FOR MICROBIOLOGY | mSystems

| Genomics and Proteomics | Research Article

Floodplain nitrifiers harbor the genetic potential for utilizing a wide range of organic nitrogen compounds

Anna N. Rasmussen,[1] Katie Langenfeld,[2] Bradley B. Tolar,[2] Zach Perzan,[2] Kate Maher,[2] Emily L. Cardarelli,[2] John R. Bargar,[3] Kristin Boye,[1] Christopher A. Francis[2,4]

AUTHOR AFFILIATIONS See affiliation list on p. 18.

ABSTRACT Organic compounds such as urea and cyanate can serve as nitrogen (N) sources for nitrifying microorganisms, including ammonia-oxidizing archaea (AOA) and bacteria (AOB), complete ammonia-oxidizing (comammox) bacteria, and nitrite-oxidizing bacteria (NOB). Here we investigated metagenome-assembled genomes (MAGs) for all four nitrifier guilds generated from hydrologically variable floodplain sediments of the Wind River Basin (WRB; Riverton, WY, USA) for their genetic potential to utilize organic N compounds. A vast majority of WRB nitrifier MAGs harbored urease (*ure*) and at least one urea transporter (*utp*, *urt*, *dur3*). AOA were the most abundant and phylogenetically diverse nitrifiers in WRB floodplain sediments. Several AOA MAGs encoded cyanase (*cynS*), nitrilase (*nit1*), omega-amidase (*nit2*), nitrile hydratase (*nthA*), and genes related to purine degradation, including biuret hydrolase (*biuH*), oxamic transcarbamylase (*allFGH*), and catabolic carbamate kinase (*allK*). AOA often encoded an uncharacterized amidohydrolase collocated with *biuH*, rather than allophanate hydrolase (*atzF*). A small number of AOA encoded *atzF*, functioning in an unknown pathway. AOB and comammox were of relatively low abundance and taxonomic diversity and were present only at certain depths in WRB; however, they encoded triuret/biuret degradation genes (*trtA*, *biuH*, and *atzH*), and in comammox, these genes were also collocated with *allFGHK*. The genetic potential of ammonia oxidizers in the WRB floodplain suggests that organic N may support nitrification in this system. The proposed pathways for utilizing purine degradation products other than urea potentially expand the known metabolic capabilities of AOA, AOB, and comammox bacteria and reveal the possibility for cryptic N cycling between microbial community members.

IMPORTANCE Floodplains are critical ecosystems where terrestrial and riverine systems meet. Floodplain sediments experience many, sometimes dramatic, changes in moisture and oxygen concentrations because of changes in water table height, flooding, and drought, leading to active microbial cycling of contaminants and nutrients. Nitrogen is one such nutrient that is not only essential for the building blocks of life but can also be used as an energy source by some microorganisms. Microorganisms that oxidize ammonia and nitrite are a crucial part of the nitrogen cycle and can lead to eventual nitrogen loss from a system. Investigating the genes present in microorganisms responsible for nitrification in a dynamic floodplain suggests that organic nitrogen—from decaying plants or potentially other sources, such as fertilizers, grazing livestock feces, or contaminants (e.g., pesticides, pharmaceuticals)—is an important nitrogen source to these microorganisms. This study identifies genes not previously described in nitrifying microorganisms, expanding their potential metabolic substrates.

KEYWORDS nitrification, metagenomics, floodplain, sediments, nitrogen metabolism, organic nitrogen

Editor Jorge L. M. Rodrigues, University of California, Davis, Davis, California, USA

Address correspondence to Christopher A. Francis, caf@stanford.edu.

The authors declare no conflict of interest.

See the funding table on p. 18.

Received 13 June 2025
Accepted 18 September 2025
Published 13 October 2025

Floodplains are dynamic ecosystems where riverine and terrestrial systems intersect. Floodplains experience hydrological shifts, such as changes in water table height, flooding, and drought. The resulting fluctuations in sediment moisture and saturation typically drive key geochemical transformations and subsurface exchanges of water, nutrients, and other compounds across different sediment layers (1–7). Floodplains can contain high concentrations of organic nitrogen (N), and the cycling of this N is important as N is an essential element for life, can be a limiting nutrient, or become a pollutant at high concentrations (8). Nitrification, the oxidation of ammonia to nitrate via nitrite, is a critical step in the N cycle linking fixed N to N-loss processes. There are several guilds of microorganisms responsible for nitrification, including ammonia-oxidizing archaea (AOA), ammonia-oxidizing bacteria (AOB), complete ammonia-oxidizing bacteria (comammox), and nitrite-oxidizing bacteria (NOB).

In the western USA, the prevalence of nitrifier populations, particularly ammonia oxidizers, has recently been investigated in a wide range of floodplain systems. A metagenomic and metatranscriptomic study of floodplain sediments of the East River (ER; near Crested Butte, CO, USA) found genes encoding nitrification enzymes (ammonia monooxygenase and nitrite oxidoreductase) to be some of the most highly transcribed genes despite recovering a low diversity of nitrifier metagenome-assembled genomes (MAGs) (9). In the neighboring Slate River (SR; near Crested Butte, CO, USA), comammox, oligotrophic-adapted AOA, and a putative NOB sister clade to the *Nitrospiraceae* were the numerically dominant nitrifiers present in MAGs from floodplain sediments (10). A study of ammonia monooxygenase subunit A (*amoA*) genes across five floodplain sediment profiles spanning a 900 km north–south transect of the intermountain western USA (WY, CO, NM, US) found AOA to be incredibly diverse and numerically dominant over AOB (11). Based on 16S rRNA gene amplicon libraries from Wind River Basin (WRB; near Riverton, WY, USA) floodplain sediments, microbial communities include diverse AOA and AOB populations and are generally structured by depth, remaining persistent over time despite seasonal changes in water table height (12). The AOA communities in WRB floodplain sediments are structured by both sediment moisture (11, 13) and depth-associated changes in lithology (12). Beyond the USA, several studies in the Amazon River floodplain have proposed a link between nitrification and N-dependent methanotrophy (14–16), creating further potential links between N and carbon cycling.

Nitrifying microorganisms use N as both an energy source and for building biomass, and some can utilize organic N compounds to meet their N needs. Urea and cyanate can both directly and indirectly provide N for ammonia oxidizers (17–20) and nitrite oxidizers (21). Degradation products from organic N compounds can be exchanged between different guilds of nitrifiers through reciprocal feeding (i.e., between ammonia and nitrite oxidizers) and cross-feeding with other microbial community members. For example, NOB catabolizes cyanate or urea to meet cellular N-demand (17) and may also supply ammonia to ammonia oxidizers, which in turn produce nitrite that can be oxidized by NOB (18, 22). A recent study also proposes cryptic N-cycling in oceans between abundant microbial community members, where *Prochlorococcus* and AOA exude purines and pyrimidines that are degraded by SAR11 to urea, which can then serve as a N-source for AOA, *Prochlorococcus*, and other microbial community members (23). Remineralization of polyamines by heterotrophic community members also likely allows putrescine-derived N to support nitrification in marine environments (24).

The metabolic potential to utilize organic N can benefit nitrifiers in several ways, by allowing them to thrive in environments with low ammonia concentrations or by creating separate niches for different nitrifier guilds. For example, urea-fed systems can allow the co-existence of comammox and NOB *Nitrospira*, or AOA and AOB, compared to systems with high ammonia amendments (25, 26). Urea and cyanate degradation pathways are encoded by many nitrifiers: for example, a comparative genomics analysis of 289 high-quality genomes found 50% of AOA, 60% of AOB, and 80% of comammox encoded genes for urea transport, urease, and accessory proteins (27). In another study of 70 representative nitrifier genomes, ~50% encoded genes related to urea uptake and degradation, and ~12% encoded cyanate lyase (*cynS*), while known genes involved in the degradation of polyamines, taurine, glycine betaine, and methylamines were completely absent (28). However, the possible organic N sources directly used by nitrifiers continue to expand to include sewage-, farming-, and industrial-related contaminants, as well as other organic matter breakdown products. For example, a recent study shows that some comammox, and perhaps AOB, can use guanidine—a nitrogen-containing compound formed by degradation of compounds such as guanylurea, metformin, and cyanoguanidine—as a reductant, an energy source, and an N source (29). A putative nitrilase (NIT1) is mostly conserved in AOA (30), while a nitrile hydrolase (NTH) (13) and a putative nitrilase/omega amidase (NIT2) (30) are encoded by some AOA, supporting their potential degradation of nitriles—a broad class of naturally occurring and man-made organic compounds containing a cyano functional group—and/or dicarboxylic acid monamides to produce ammonia. Another recent study found the genetic potential in comammox bacteria for degrading polyurea molecules, triuret (carbonyldiurea), and biuret (carbamylurea) (10), which are common impurities in urea fertilizers and breakdown products from oxidative purine and uric acid degradation (31–35). Laboratory incubations of forest soils have found that triuret- and biuret-derived N can support nitrification, albeit at much slower rates than for urea-fertilized soils (36–38).

Systematic studies of environments rich in organic nitrogen but with potentially variable inorganic N sources, such as natural floodplains (39–41), can help identify which organic N compounds may be used directly by nitrifying microorganisms. In this study, we investigate nitrifier diversity and genetic potential to utilize alternative sources of ammonia in hydrologically variable floodplain sediments. We analyzed MAGs generated from the WRB at three sites (KB1, Pit2, and PTT1; Fig. 1) with generally similar sediment geochemical composition but varying depths to gravel bed/capillary fringe, sampled in different years (2015, 2017, and 2019, respectively).

RESULTS

A total of 9,989 MAGs (bins > 50% complete and <10% contamination) were generated from 68 floodplain metagenomes from three nearby sites in the WRB. After dereplication

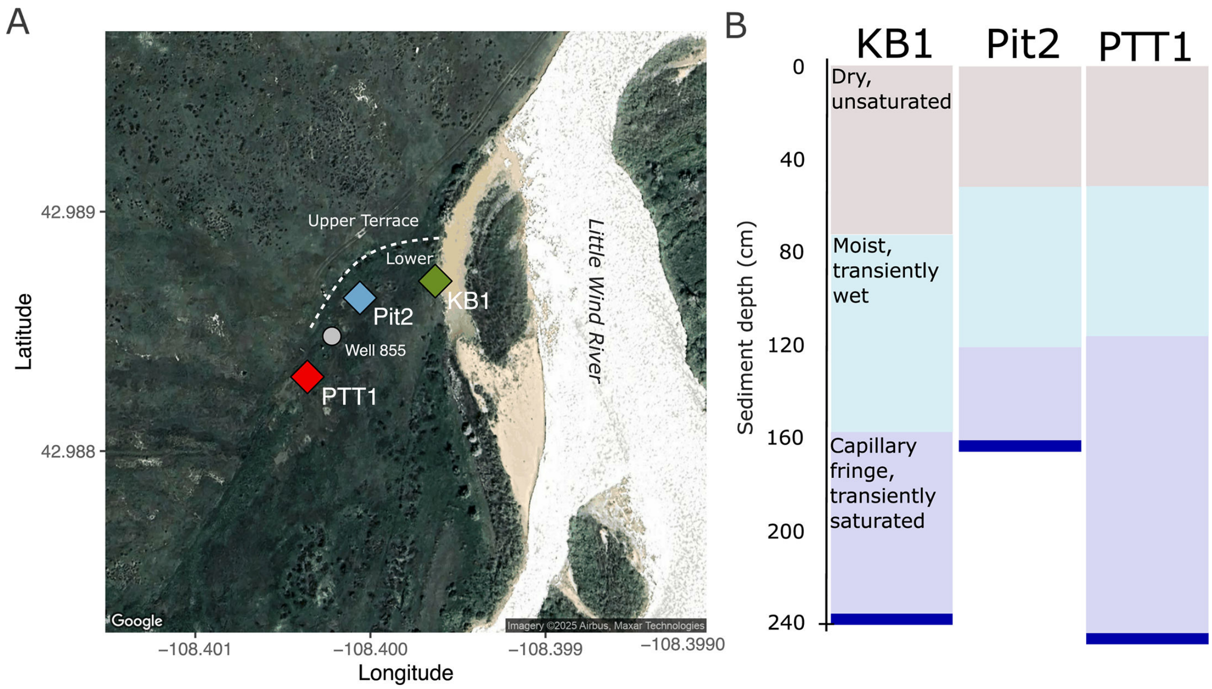

FIG 1 (A) Map of sampling sites in the Wind River Basin (WRB) near the Little Wind River and Wind River, Wyoming, USA (Map data ©2025 Google ©2025 Airbus, Maxar technologies). (B) Schematic of general sediment conditions at each site.

at 98% average nucleotide identity (ANI), a total of 3,874 MAGs formed a non-redundant data set of microbial "lineages" present in the site. The non-redundant MAG data set recruited 13.5%–57.4% (mean 43.8%) of metagenome reads, with the lowest recruitment occurring in the shallowest samples (Fig. S1). MAGs originated from over 60 phyla, with the highest number coming from *Actinomycetota* (formerly *Actinobacteria*, n = 2,066) and *Pseudomonadota* (formerly *Proteobacteria*, n = 2,065). MAGs for several nitrifier guilds were recovered, including AOA (n = 189), AOB (n = 11), comammox bacteria (n = 6), and NOB (n = 68). Additionally, two non-AOA *Nitrososphaeria* MAGs similar to those reported previously (13) were recovered from the "JACPRH01" family (*Nitrososphaerales*) (Fig. 2). No anammox MAGs were recovered. All together, 63 nitrifier lineages spanning 22 genera were recovered. Nitrifiers were present in 67 of 68 samples at an average abundance of 44 reads per kilobase of genome per gigabase of metagenome (RPKG; range = 4.5 to 184 RPKG). Nitrifier richness (total number of observed MAGs present) at each site was similar (n = 51, 53, and 56 at PTT1, KB1, and Pit2, respectively); however, nitrifier richness

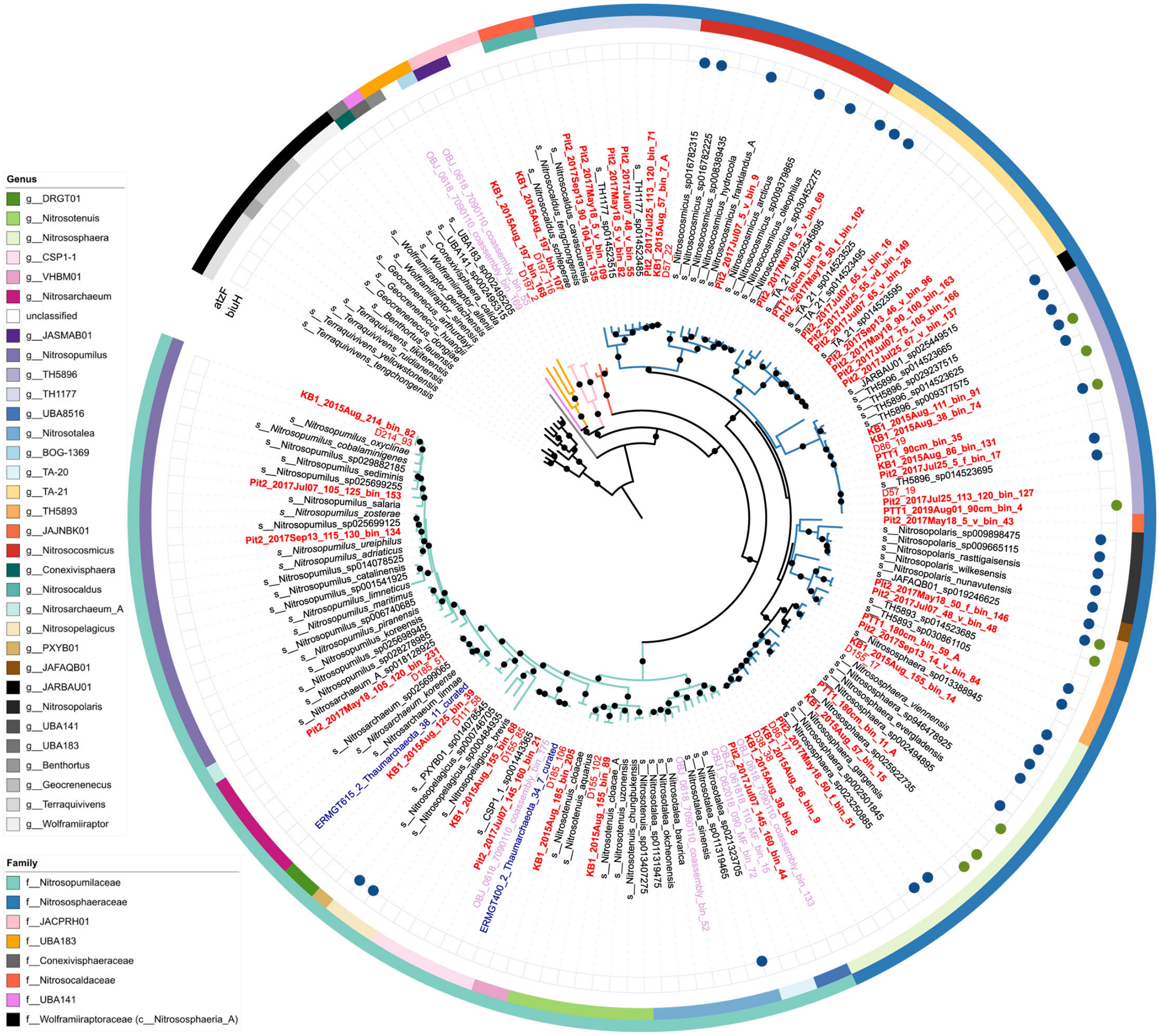

FIG 2 Concatenated ribosomal tree made using IQ-TREE2 with model LG + F + R7 for select *Nitrososphaerales* MAGs, including all non-redundant plus *atzF*- or *biuH*-encoding *Nitrososphaeria* MAGs generated from WRB (red), Slate River (SR; light purple), and East River (ER; blue), as well as NCBI type material (italics) and *atzF*- or *biuH*-encoding GTDB species representatives. MAGs generated in this study are in bold. External circles indicate the presence of the *biuH* and *atzF* genes. Outer ring color indicates GTDB-assigned family, and the inner ring indicates genus. Black dots indicate nodes with ≥ 90% bootstrap support. Tree rooted with *Nitrososphaeria_A*.

per sample (median = 16) varied by depth with the deepest sediments having the lowest richness (Fig. 3).

Nitrifier distribution was structured by depth and site in both unconstrained and constrained ordinations (Fig. S2). In a Constrained Analysis of Principal Coordinates (CAP), depth and site explained 24.3% of community variation (ANOVA, $P < 0.001$) with depth having the larger marginal effect (14.2%, ANOVA, $P < 0.001$) followed by site (10.1%, ANOVA, $P < 0.001$) (Fig. S2B and C). Despite some site heterogeneity in nitrifier communities, similar distribution patterns at the family and guild level were observed at all three sites (Fig. S2). Generally, shallower depths (0 to ~100 cm) were numerically dominated by AOA from the *Nitrososphaeraceae* family (1,731 RPKG) and NOB from the "UBA8639" family (*Nitrospira* lineage IV; 330 RPKG), in contrast to deeper depths (~100

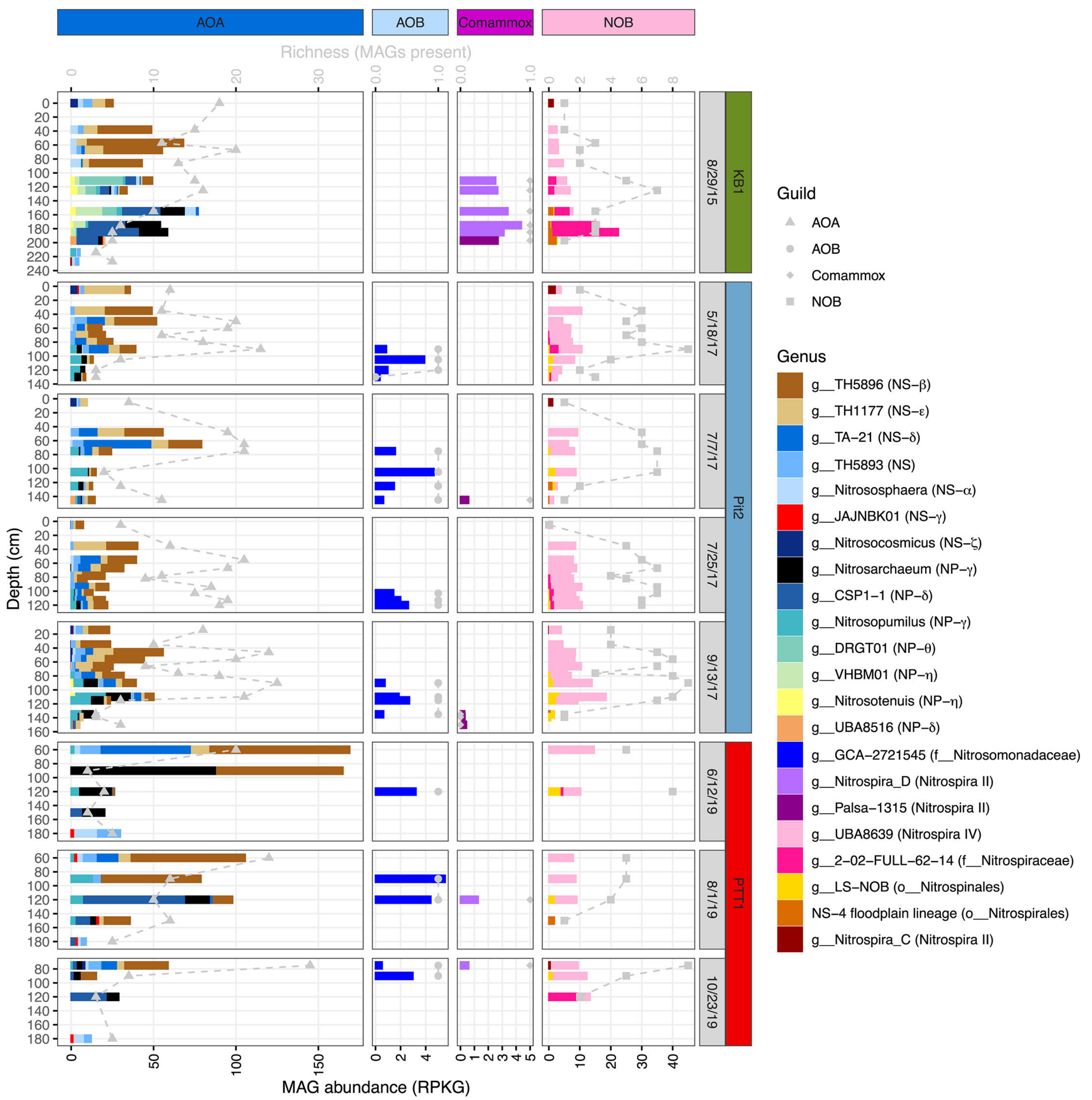

FIG 3 Relative abundance and richness of nitrifier genera (x-axis) at each depth sampled (y-axis). Relative abundance is displayed as bar plots in reads per kilobase of genome per gigabase of metagenome (RPKG), and richness is displayed as gray dashed lines and points in observed MAGs present. Both the x-axis and y-axis vary between panels. The relevant order, family, *Nitrospira* lineage, or AOA *amoA*-defined subgroup (42; NP = *Nitrosopumilaceae*, NS = *Nitrososphaeraceae*) is indicated in the parenthesis next to the genus names.

cm to 234 cm), which contained a broader diversity of nitrifiers at the family and guild levels, including AOA from the *Nitrosopumilaceae* (741 RPKG); established and putative NOB from the *Nitrospiraceae* (78 RPKG), *Nitrospinales* (31 RPKG), and "NS-4" (*Nitrospirales*; 8 RPKG); comammox from both *Nitrospira_D* and "Palsa-1315" (*Nitrospiraceae*; 22 RPKG); and AOB from the *Nitrosomonadaceae* (43 RPKG; Fig. S2).

Nitrifier taxonomic diversity

AOA were the most abundant and diverse in terms of richness of the nitrifiers throughout the sediment column at all three sites sampled (Fig. 3). We recovered medium- to high-quality AOA MAGs representing 45 lineages from 14 genera after dereplication at 98% ANI (Table S1). AOA were depth differentiated, with organisms from the *Nitrososphaeraceae* numerically dominating in the upper (< ~100 cm) sediment depths transitioning to *Nitrosopumilaceae* numerically dominating in deeper (> ~100 cm) depths (Fig. S2). The most abundant and widely distributed of the 7 *Nitrososphaeraceae* genera included "TH5896" (911 RPKG), "TH1777" (301 RPKG), "TA-21" (279 RPKG), and "TH5893" (125 RPKG) (Fig. 3). Of the low-abundance *Nitrososphaeraceae*, *Nitrososphaera* (82 RPKG) were cosmopolitan across the sediment column, in contrast to *Nitrosocosmicus* (15 RPKG) and "JAJNBK01" (18 RPKG), which were generally present only in the shallowest or deepest sediments, respectively. *Nitrosopumilaceae* was most abundant and had the highest richness at KB1, with the genera "DRGT01" and "VHBM01" present only at KB1. Among the *Nitrosopumilaceae* genera, *Nitrosarchaeum* was the most abundant overall (285 RPKG) and was found at all three sites; however, at both KB1 and PTT1, "CSP1-1" (234 RPKG) was the most abundant at deeper depths, in contrast to Pit2, where *Nitrosopumilus* (82 RPKG) was the most abundant (Fig. 3).

NOB were also cosmopolitan in WRB floodplain sediments (Fig. 3). Established and putative NOB MAGs originated from five genera from the *Nitrospirales* and *Nitrospinales* orders, represented by 15 lineages after dereplication. The vast majority (75%) of NOB MAGs originated from the Genome Taxonomy Database (GTDB)-defined genus UBA8639 within the UBA8639 family (*Nitrospira* lineage IV). The UBA8639 genus was present at most depths throughout the floodplain sediment column at all three sites and consisted of 11 lineages after dereplication with different depth distributions, including one lineage that was absent from KB1 (Fig. S3). Other established NOB include LS-NOB (*Nitrospinales*) that was present in deep sediments and *Nitrospira_C* (*Nitrospira* lineage II) that was present in shallow sediments. Uncultured, putative NOB were present in deeper depths and originated from "2-02-FULL-62-14" (*Nitrospiraceae*) and the same NS-4 (*Nitrospirales*) lineage found in SR floodplain sediments (Fig. S4) (10). In contrast to AOA and NOB, bacterial ammonia oxidizers were present at low abundance, occurred only at deeper depths, and consisted of a single lineage of comammox clade A (*Nitrospira*_D; *Nitrospira* lineage II), comammox clade B (Palsa-1315; *Nitrospira* lineage II), and AOB ("GCA-2721545" genus *Nitrosomonadaceae*) (Fig. 3; Fig. S4 and S5). Further details on bacterial nitrifier diversity and distributions can be found in the Supplemental Results, subsection "Bacterial nitrifier MAGs."

Osmoregulation genes

Genes associated with different osmoregulation strategies were also present in nitrifier MAGs. Generally, AOA and AOB lacked genes for uptake or synthesis of compatible solutes, although many of these genes were present in NOB and comammox MAGs (Fig. S6). AOA and bacterial nitrifiers generally encoded different sodium/proton antiporters, mechanosensitive channels, and potassium uptake systems (Fig. S6). Few bacterial nitrifiers encoded aquaporins relative to archaea; most AOA had at least one aquaporin gene, and some encoded two (Fig. S6). A more detailed description of osmoregulation genes can be found in the Supplemental Results.

Dissolved inorganic N uptake and utilization

Ammonium transporter genes (*amt*) were annotated in most (82%) nitrifier lineages excluding the AOB lineage (Fig. 4; Fig. S7). Over half (59%) of the *amt*-encoding lineages encoded two or more *amt* genes. Based on gene phylogeny, AOA *amt* genes can be classified as encoding either a high-affinity transporter or a low-affinity transporter (43), which we refer to as Amt1 and Amt2, respectively (44–47). A total of 26 AOA lineages encoded the low-affinity *amt1*, and 25 AOA lineages encoded the high-affinity *amt2*, with 16 encoding both (Fig. S8). AOA MAGs harbored the expected ammonia monooxygenase genes (*amoABC*), which were absent from the two non-AOA *Nitrososphaerales* MAGs (Fig. 4; Fig. S8). AOB MAGs contained genes for ammonia oxidation (*amoABC*, *hao*) (Fig. 4; Fig. S8). Of the two proposed comammox lineages present in WRB, *Nitrospira_D* MAGs encoded *amoABC*, *hao*, and *nxrAB*, in contrast to the less complete Palsa-1315 MAG, which lacked these genes (Table S1; Fig. S4). Despite lacking these nitrification genes, the Palsa-1315 MAG was closely related to comammox MAGs from SR and ER (Fig. S4) and harbored genes for utilizing biuret/triuret (Fig. 4, discussed in detail below), supporting our assertion that it represents a comammox lineage. The *nxrAB* genes had a patchy distribution in both established and putative NOB MAGs from WRB and were missing from 67% of representative MAGs (Fig. S8). The nitrite/nitrate transporter (*narK*) was encoded by most (79%) *Nitrospirales* NOB MAGs and the Palsa-1315 MAG. Additionally, the UBA8639 (*Nitrospira* lineage IV) and LS-NOB (*Nitrospinales*) MAGs encoded nitrite transporter, *nirC*. UBA8639 MAGs harbored genes for assimilatory nitrite reduction (*nirA*) as did LS_NOB (*nirA*, *nasBDE*) (Fig. 4; Fig. S8).

Proposed pathways for utilizing purine degradation products

Urea is a common product of purine and pyrimidine degradation. Most (77%) ammonia oxidizer MAGs along with 40% of NOB lineages from the WRB harbored at least one urease subunit (Fig. 4; Fig. S8). Three types of urea transporters were present and differently distributed across nitrifier guilds (Fig. 4 and 5). The ABC urea transport system (*urtABCDE*) was encoded by both comammox lineages (*Nitrospira_D*, Palsa-1315) and *Nitrospiraceae* NOB (2-02-FULL-62-14, *Nitrospira_C*) (Fig. 4; Fig. S8). A urea transporter (*utp*) was found throughout the *Nitrososphaeraceae* family and in *Nitrospira_C* (Fig. 4; Fig. S8). Lastly, the urea-proton symporter (DUR3) was encoded by a total of five AOA lineages from the *Nitrososphaeraceae* (*Nitrosocosmicus*, *Nitrososphaera*, TA-21, TH5893, TH5896) and *Nitrosopumilaceae* (*Nitrosopumilus*, VHBM01) (Fig. 4; Fig. S8) and four UBA8639 lineages (Fig. S8). Although nine UBA8639 MAGs encoded DUR3 in total, urease or other urea transporter (*utp*, *urt*) genes were completely absent (0/51 MAGs; Fig. S8).

Genes related to guanidine degradation (i.e., guanidinase, guanidine carboxylase, carboxyguanidine deiminase, and APC superfamily permease) were absent from all WRB nitrifier MAGs based on a *blastp* search (e-value cutoff 1e-20). However, MAGs from all three ammonia oxidizer guilds encoded genes annotated as allophanate hydrolase (*atzF*) (Fig. 4 and 5). The *atzF* sequences from AOB MAGs did not fall into a clade with the *atzF* of guanidine-degrading AOB and comammox (*Nitrosomonas*, *Nitrosospira*, and *Nitrospira*) but rather were more closely related to *atzF* sequences from other *Nitrosomonadaceae* and *Herbaspirillum* (Fig. S9). In AOB from WRB, *atzF* was collocated with genes encoding biuret hydrolase (*biuH*), a putative triuret hydrolase (*trtA*) based on phylogeny (Fig. S10), a putative carboxybiuret decarboxylase (*trtB*) (Fig. S11), and an ABC nucleoside transporter (*bmpA-nupABC*) (Fig. 6). Generally, triuret degradation requires two isochorismatase-like hydrolases (*trtA*, *biuH*), a decarboxylase (*trtB*), and an amidohydrolase (*atzF*) (31); thus, this contig harbored a complete pathway for triuret degradation. Nearby on the same contig was a complete urease (*ureABCDEFG*) cassette.

Similar to the pathway observed in AOB, *Nitrospira_D* MAGs harbored *atzF* collocated with *biuH*, putative *trtA*, and *bmpA-nupABC* (Fig. S12). Additionally, genes encoding the oxalurate degradation pathway were located next to the triuret degradation pathway, including *allFGH* (formerly *fdrA/yahF*, *ylbE/DUF1116*, and *ylbF/DUF2877* [48]) and carbamate kinase (*allK*, formerly *arcC/ybcF* [49]) (Fig. S12), which are discussed in

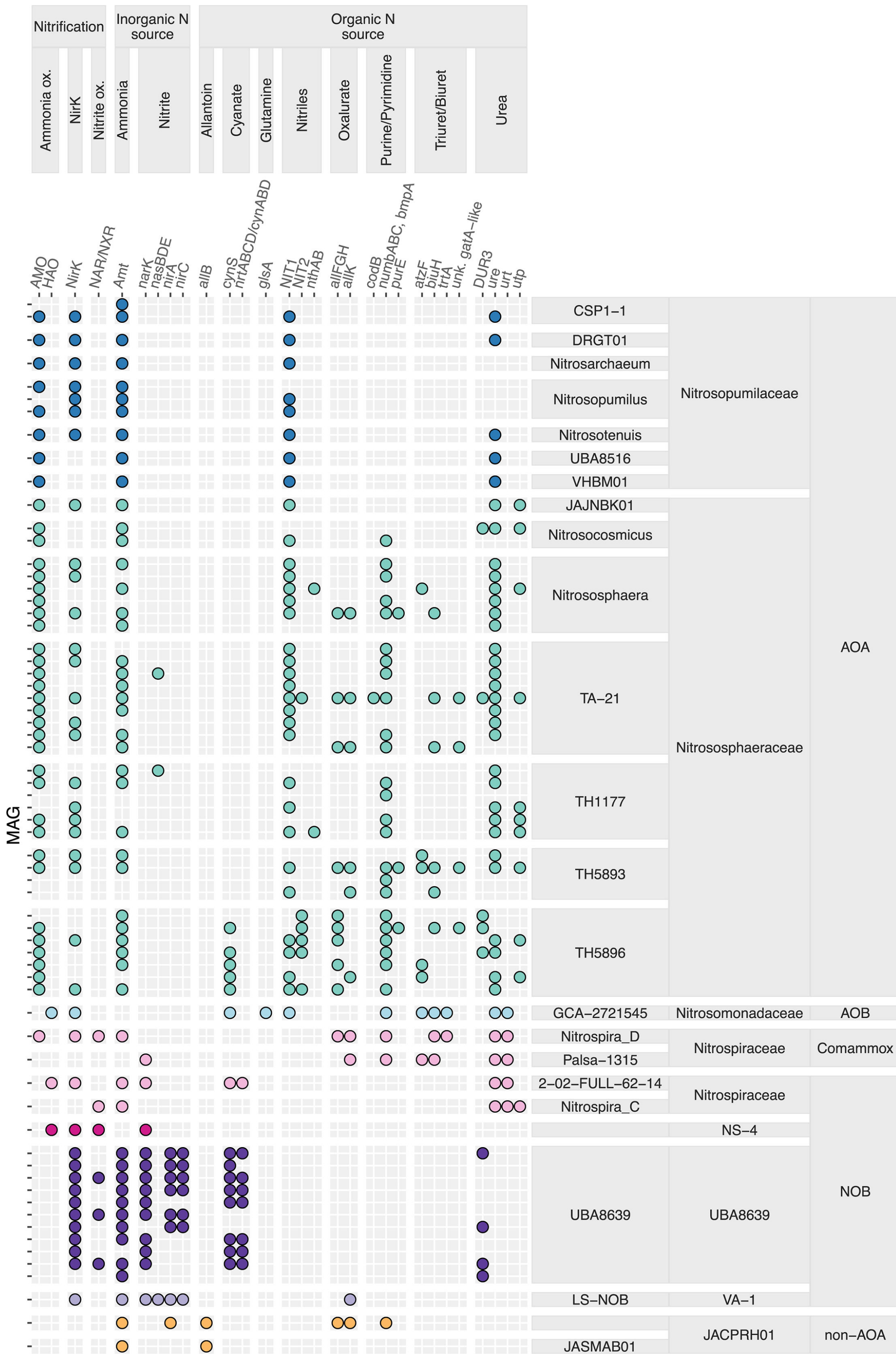

FIG 4 N cycling gene presence-absence in nitrifier lineage representatives. Genes include: ammonia monooxygenase (AMO: *amoABC*), hydroxylamine oxidoreductase (*hao*), nitrate reductase/nitrite oxidoreductase (NXR/NAR: *nxrAB*), nitrite reductase (*nirK*), ammonium transporter (*amt*), nitrite transporter (*nirC*), NNP family nitrate/nitrite transporter (*narK*), nitrite reductase (*nirA, nasBDE*), allantoinase (*allB*), cyanate lyase (*cynS*), nitrite/nitrate/cyanate transporter

(Continued on next page)

Fig 4 (Continued)

(*nrtABCD/cynABD*), glutaminase (*glsA*), nitrilase (*nit1*), nitrile hydratase (*nthA*), omega amidase (*nit2*), oxamic transcarbamylase (*allFGH*), carbamate kinase (*allK*), cytosine permease (*codB*), ABC-type nucleoside transporter (*bmpA-nupABC*), 5-carboxyaminoimidazole ribonucleotide mutase (*purE*), allophanate hydrolase (*atzF*), biuret hydrolase (*biuH*), triuret hydrolase (*trtA*), uncharacterized *gatA*-like amidohydrolase, urease (*ure*), urea transport system (*urt*), urea transporter (*utp*), and urea-proton symporter (*dur3*).

further detail in the Supplemental Results. Oxalurate degradation is the final step in the oxamate branch for the ALL allantoin degradation pathway (50). The Palsa-1315 MAG from WRB also encoded *biuH* and *atzF*. Known genes for upstream purine degradation were absent from both AOB and comammox MAGs. There was general gene synteny of the triuret degradation pathway between bacterial nitrifiers from the WRB; however, comammox contigs lacked *trtB* and also encoded *allFGHK* (Fig. 6; Fig. S12). There was strong gene synteny between *Nitrospira_D* and Palsa-1315 genomes harboring this pathway, including in the enriched *Ca*. Nitrospira nitrificans COMA2 strain (51) (Fig. S12).

A total of 12 AOA MAGs encoded genes annotated as *atzF*, including MAGs from three distinct genera: *Nitrososphaera*, TH5893, and TH5896. Contigs harboring *atzF* were generally short and encoded genes for uncharacterized and hypothetical proteins (Fig. S13). Additionally, of the WRB AOA encoding *atzF,* only three also encoded *biuH* (Fig. 2 and 4). Only 2 out of 554 GTDB species representatives within the *Nitrososphaeria* and 1 River Thames AOA MAG encoded *atzF* based on a *blastp* search (Fig. 2, e-value cutoff 1e-40). Three WRB AOA harbored multiple copies of *atzF*, sometimes located on the same contig (Fig. S13). The amino acid sequences of AtzF from AOA fell into an archaeal clade most closely related to bacterial AtzF and not other amidohydrolases found in other purine catabolism pathways (Fig. S9). Compared to structurally characterized AtzF from

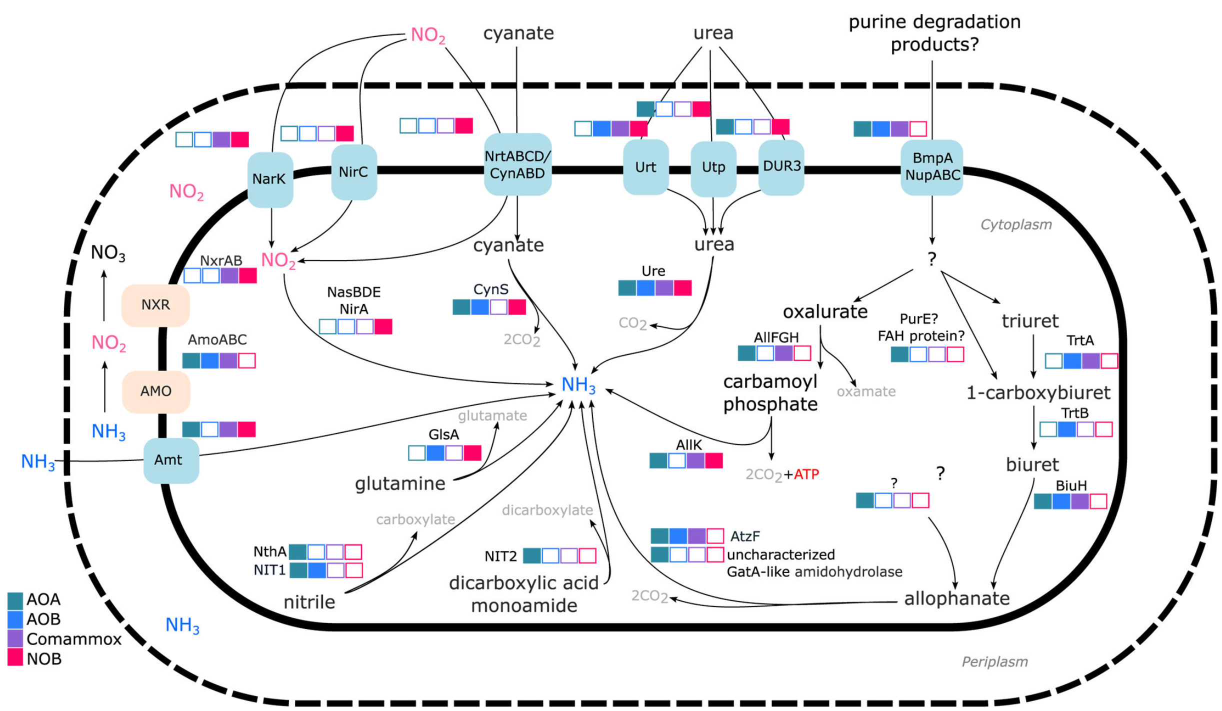

FIG 5 Schematic of predicted N cycling metabolisms in WRB nitrifier MAGs. Filled boxes indicate the presence of a given gene in at least one MAG of a specified nitrifier guild. Select functional genes were used to represent metabolic processes, including ammonium transport (Amt), ammonia oxidation (AmoABC), nitrite oxidation (NxrAB), nitrite transport (NirC), nitrite/nitrate transport (NarK), assimilatory nitrite reduction (NirA, NasBDE), nitrite/nitrate/cyanate transport (NrtABCD/CynABD), cyanate hydrolysis (CynS), urea transport (Urt, Utp, DUR3), urea degradation (Ure), glutamine deamination (GlsA), nitrile degradation (NIT1, NthA), dicarboxylic acid degradation (NIT2), ABC-type nucleoside transport (BmpA-NupABC), triuret hydrolysis (TrtA), carboxybiuret decarboxylation (TrtB), biuret hydrolysis (BiuH), allophanate hydrolysis (AtzF, uncharacterized GatA-like amidohydrolase), oxalurate degradation (AllFGH), and carbamate degradation (AllK). Note that the orientation of AMO has yet to be confirmed.

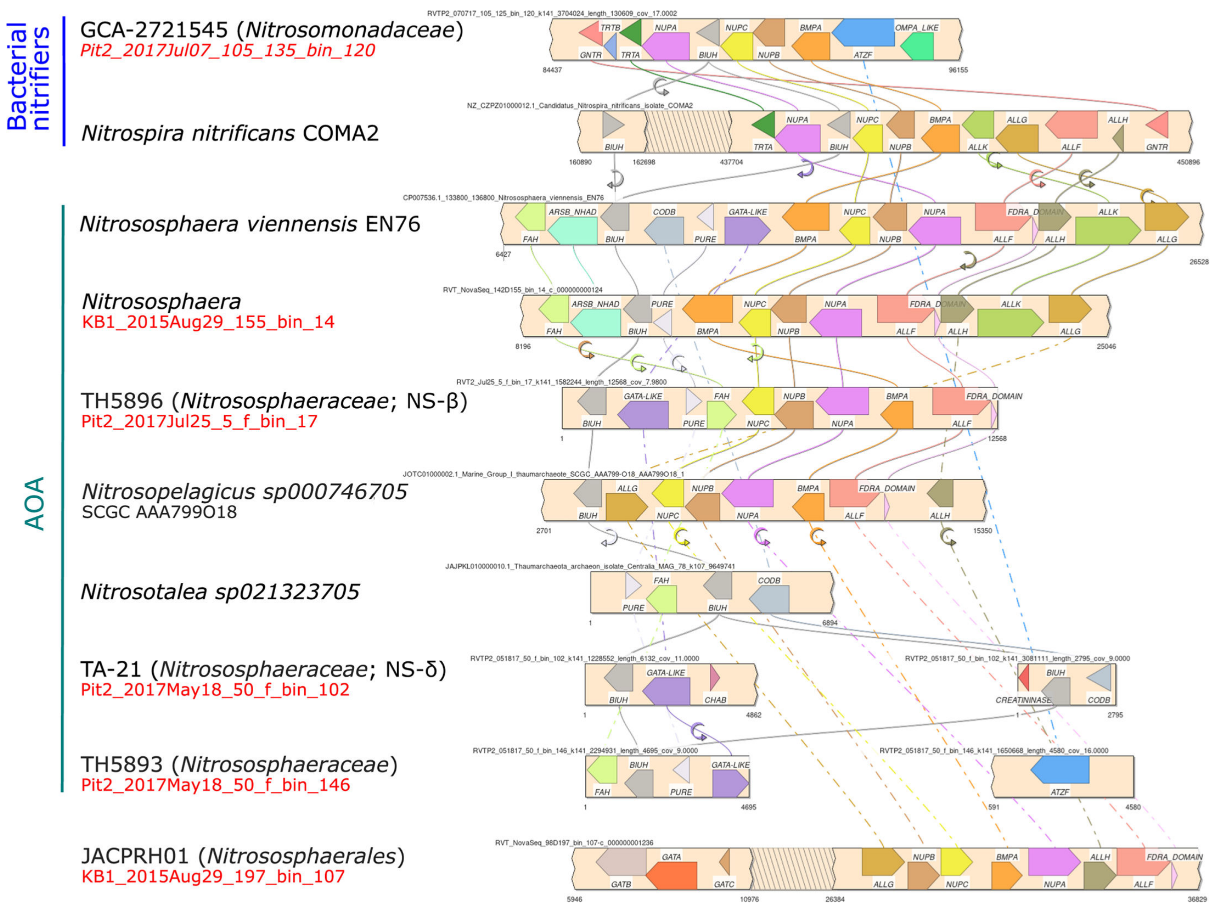

FIG 6 Gene synteny of *biuH*-harboring contigs in bacterial and archaeal ammonia-oxidizer genomes. Annotated genes include allophanate hydrolase (*atzF*), biuret hydrolase (*biuH*), triuret hydrolase (*trtA*), carboxybiuret decarboxylase (*trtB*), ABC-type nucleoside transporter (*bmpA-nupABC*), oxamic transcarbamylase (*allFGH*), catabolic carbamate kinase (*allK*), *gntR* family transcriptional regulator, cytosine permease (*codB*), intermolecular transferase 5-(carboxyamino)imidazole ribonucleotide mutase (*purE*), fumarylacetoacetate hydrolase family protein (FAH), creatininase, and an uncharacterized amidohydrolase (*gatA*-like). Extended data in Fig. S12 and S15. WRB MAG names in red.

Pseudomonas sp. 47660, *Kluyveromyces lactis*, and *Granulibacter bethesdensis*, the AOA AtzF sequences contained several insertions and a truncated C-terminus (Fig. S14A).

In total, 19 AOA MAGs from the WRB encoded genes that were annotated as *biuH* (Fig. 4; Fig. S8). These *biuH* sequences were distinct from other isochorismatase-like hydrolases, such as *trtA* and guanylurea hydrolase (*guuH*) (52) (Fig. 7; Fig. S10), and were in agreement with findings in a previous study identifying a high-confidence *biuH* sequence from *Nitrososphaera* (53). In a midpoint-rooted tree, AOA *biuH* sequences formed a cluster containing archaeal and bacterial *biuH* sequences, including sequences from the AOB *Nitrosospira*, that was sister to a bacterial *biuH* cluster containing sequences from many bacterial genera including *Herbaspirillum*, *Nitrospira*, and members of the *Nitrosomonadaceae* (Fig. S10). Compared to the structurally characterized BiuH enzyme of *Herbaspirillum* sp. strain CAH-3 (54) and *Rhizobium leguminosarum* bv. *viciae* 3841 (55), the AOA sequences had an extended N-terminal and several insertions (Fig. S14B). Like the AOB and comammox contigs that encoded *biuH*, AOA contigs also encoded an ABC nucleoside transporter (*bmpA-nupABC*). In contrast to bacterial ammonia oxidizers, however, AOA did not encode a collocated *atzF* and did not have strong gene synteny across genera (Fig. 6; Fig. S15). Most (68%) *biuH*-encoding AOA MAGs encoded an uncharacterized amidohydrolase annotated as a glutamyl-tRNA amidotransferase subunit A (*gatA*) next to *biuH*. This "*gatA*" diverged from the *gatA* sequence found in *gatCAB* cassette, which encodes the glutamyl-tRNA amidotransferase present in most

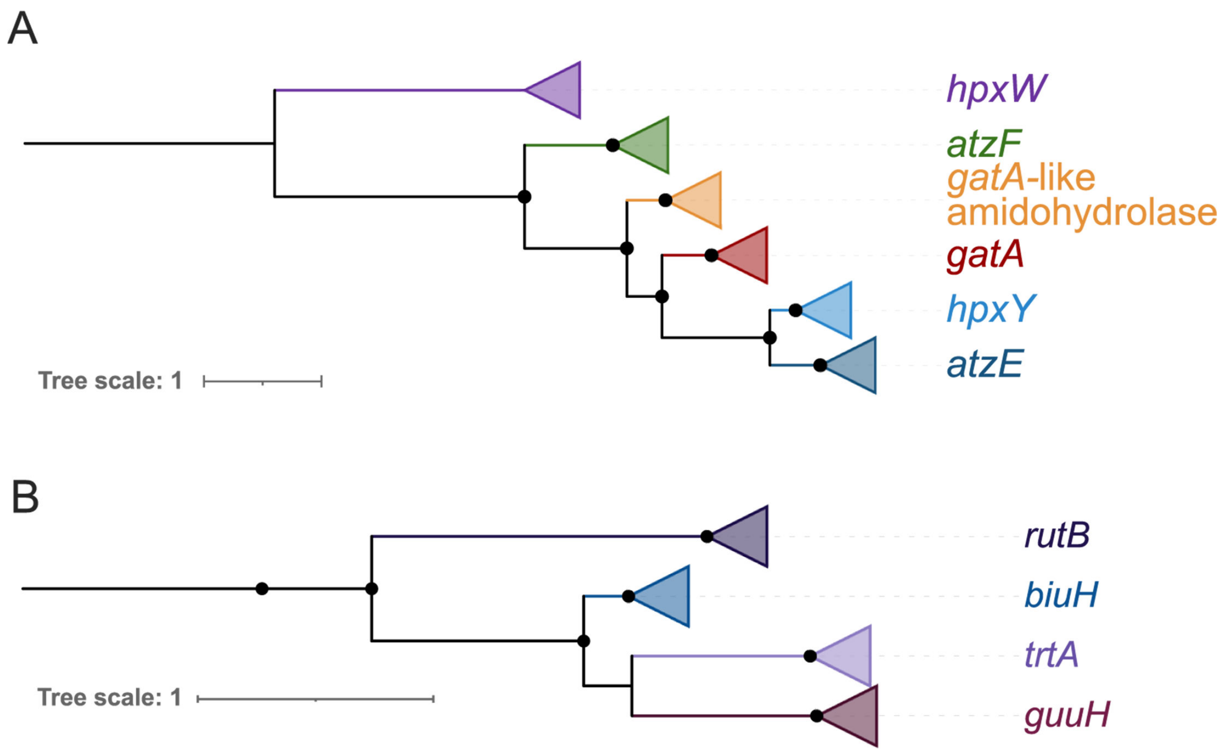

FIG 7 (A) Phylogeny of amidohydrolase genes, including allophanate hydrolase (*atzF*, green branches), carboxybiuret hydrolase (*atzE*), glutamyl-tRNA amidotransferase (*gatA*), oxamate carbamoyltransferase (*hpxY*), oxamate amidohydrolase (*hpxW*), and the uncharacterized *"gatA-like"* amidohydrolase from AOA (orange branches, based on a 533 position amino acid alignment of 150 sequences made with IQ-TREE2 model LG + G4. Extended data in Fig. S9. (B) Phylogeny of isochorismatase genes, including biuret hydrolase (*biuH*), triuret hydrolase (*trtA*), guanylurea hydrolase (*guuH*), and ureidoacrylate amidohydrolase (*rutB*), based on a 257 position amino acid alignment of 234 sequences made with IQ-TREE2 model LG + R6. Extended data in Fig. S10. The tree is pruned to exclude distantly related structurally characterized isochorismatase-family proteins. Black dots indicate bootstrap support of ≥ 90%, and trees are midpoint rooted.

archaea (56) and found in most AOA MAGs generated in this study. Additionally, "*gatA*" was phylogenetically distinct from closely related amidohydrolases in the ALL and HPX purine catabolism pathways (50), including 1-carboxybiuret hydrolase (*atzE*) and oxalurate amidohydrolase (*hpxY*) (Fig. 7; Fig. S9). Like the comammox *biuH*-harboring contigs, AOA *biuH* contigs also often encoded *allFGHK* for oxalurate degradation (Fig. 6). In several AOA, *biuH* was collocated with a fumarylacetoacetate hydrolase (FAH) family protein gene, which is essential in aromatic degradation pathways (57), and an intermolecular transferase 5-(carboxyamino)imidazole ribonucleotide mutase (*purE*) (Fig. 6; Fig. S15). A few AOA also harbored a cytosine permease (*codB*), and one WRB MAG harbored two *biuH* sequences—one located near a gene annotated as a creatinine amidohydrolase, most closely related to other creatininase-like sequences from uncultured *Nitrososphaeraceae*, but distinct from those found in cultured *Nitrosopumilaceae* and some cultured *Nitrososphaeraceae* creatininase-like sequences (Fig. S16). One of the non-AOA *Nitrososphaerales* MAGs encoded *allFGHK* and *bmpA-nupABC* on the same contig as *gatCAB* (Fig. 6; Fig. S15). No AOA MAGs encoded known genes for upstream purine degradation.

Six non-redundant AOA MAGs encoded *biuH* and were present in 85% of samples from the floodplain at an average abundance of 5.4 RPKG (range = 0.2–101 RPKG) per sample. We also identified *biuH* sequences in 27 genomes out of the 554 GTDB species representatives queried using *blastp* (e-value cutoff 1e-40), including three genomes generated from River Thames sediments, three genomes from the *Nitrosopumilaceae*, and the cultured strain *Nitrososphaera viennensis* EN76 (58) (Fig. 2). A small number of genomes encoded multiple *biuH* sequences that were not identical (Fig. S10).

Cyanate, nitrile, and glutamine degradation genes

Genes for uptake and utilization of cyanate were found in 24% of WRB nitrifier lineages. About two-thirds of UBA8639 MAGs encoded cyanase (*cynS*) and a nitrite/nitrate/cyanate ABC transporter (*nrtABCD/cynABD*), as did ~80% of 2-02-FULL-62-14 (*Nitrospiraceae*) MAGs. Several AOA (70%) from the TH5896 genus, one TA-21 MAG, and the AOB lineage encoded *cynS* (Fig. S8). The *cynS* sequences from WRB nitrifiers fell into two separate clades; one clade included sequences from many nitrifiers, including *Nitrosospira*, *Nitrosococcus*, *Nitrosomonas*, NOB *Nitrospira*, comammox *Nitrospira*, and *Nitrospina*, as well as anammox, and was related to eukaryotic *cynS*, while the other clade included *Nitrospirales*, *Nitrososphaeria,* methanotrophs, and archaeal sequences (Fig. S17). The *cynS* sequences from UBA8639 (*Nitrospira* lineage IV) MAGs fell into both clades (Fig. S18). The *cynS*-encoding nitrifier lineages were present in 84% of samples at an average total abundance of 17 RPKG per sample.

Regarding the breakdown of nitrile compounds, the gene encoding a putative nitrilase, NIT1, was present in 71% of AOA lineages and in the AOB lineage. Additionally, two AOA lineages—one from *Nitrososphaera* and one from TH1177—encoded nitrile hydratase subunit A (*nthA*), and 1 TA-21 lineage and 5 TH5896 lineages encoded a putative nitrilase/omega-amidase (NIT2). The AOB lineage and 10 MAGs from the numerically dominant NOB genus (UBA8639, *Nitrospira* lineage IV) encoded a glutaminase (*glsA*) that can convert glutamine to glutamate while releasing ammonia (Fig. 4; Fig. S8). The N-cycling gene content of WRB AOB compared to other *Nitrosomonadaceae* is discussed in further detail in the Supplemental Results.

DISCUSSION

Diverse and marine-like nitrifiers found in WRB floodplain sediments

The taxonomic diversity and depth-differentiated structure of AOA MAGs recovered in this study are in line with previous *amoA* and 16S rRNA gene amplicon studies at this site near Riverton, WY (11, 12). The AOA genera recovered in this study expand upon the MAGs reported for 2015 samples (13) to include lineages from the GTDB-defined genera UBA8516 (*Nitrosopumilaceae*), TA-21 (*Nitrososphaeraceae*), TH5893 (*Nitrososphaeraceae*), and *Nitrosocosmicus* (*Nitrososphaeraceae*). Many abundant lineages of AOA in the WRB floodplain sediments are related to *Nitrososphaeraceae* MAGs from sediments of the River Thames, including TH5896, TH5893, and TH1177. Phylogenomic reconstruction and analysis of proteome content changes indicate that lineages in the *Nitrososphaeraceae* have undergone many gene duplication and loss events, allowing for distinct and often large proteomes to emerge and for lineages to specialize to different niches selected for by the environment (59). These patterns in genome evolution could explain the prevalence of *Nitrososphaeraceae* in the dynamic WRB floodplain sediments. In addition to the diverse AOA genera, several genera of established and putative NOB from the *Nitrospirales* and *Nitrospinales*, two comammox lineages, and an AOB lineage were recovered from WRB floodplain sediments. The greater taxonomic diversity of nitrifiers and numeric dominance of AOA in the WRB is in contrast to the SR floodplain nitrifier community, which was numerically dominated by comammox bacteria, AOA adapted to oligotrophic conditions, and putative NOB from the NS-4 family (*Nitrospirales*) (10). However, like SR nitrifier MAGs, WRB MAGs encoded the genetic potential to use many different organic N compounds as N and/or energy sources.

Marine and estuarine-like nitrifier lineages were found in deeper depths of WRB floodplain sediments. For example, *Nitrosopumilaceae*, including *Nitrosopumilus* and *Nitrosarchaeum*, were the most abundant AOA in deeper depths of WRB sediments. The NOB lineage, UBA8639 (*Nitrospira* lineage IV), was cosmopolitan in WRB, and LS-NOB (Clade 2 *Nitrospinae*) was found in deeper depths. Both of these NOB groups tend to be associated with marine environments (60–62). The AOB in WRB were also closely related to marine lineages (Fig. S5). This could be due to high sulfate concentrations in groundwater (~4.5–9 g/L) or higher salinity in the transiently saturated and transition zones (~6.5–11.5 ppt) of WRB soils (12, 63, 64). Nitrifier MAGs encoded several different strategies for osmoregulation (compatible solutes versus salt-ion exchange) that varied between different guilds and genera, potentially allowing organisms to adapt to the dynamic floodplain and variable osmotic pressure outside the cell.

Putative novel pathways indicate additional purine degradation products could support ammonia oxidation

A common degradation product from both purine and pyrimidine catabolism is urea, which has been established as an important energy and N-source for nitrifiers in a range of environments (17, 19, 20, 65). Indeed, urease was encoded by a little over half of the WRB nitrifier MAGs presented in this study and was found across all four nitrifier guilds (28). However, outside of urea, upstream purine degradation products can supply N to microorganisms (66), and this study suggests that they may also support nitrification. Purines can be completely degraded through several different aerobic and anaerobic pathways, generally first metabolized to xanthine, followed by conversion to key intermediates urate and allantoin (50, 66, 67). Allantoin can then be metabolized aerobically through allantoate to glyoxylate and ammonia, or anaerobically through glyoxylate and oxalurate to 2-phosphoglycerate, urea, oxamate, and ammonia (50). Here, we identified downstream purine degradation pathways, such as oxalurate and/or triuret/biuret degradation, in AOA, AOB, and comammox (Fig. 4).

The AOB from the WRB harbored genes comprising a triuret degradation pathway similar to that described in *Herbaspirillum* (31), where triuret is hydrolyzed to carboxybiuret (*trtA*), then decarboxylated to biuret (*trtB*), hydrolyzed to allophanate (*biuH*), and finally hydrolyzed to ammonia (*atzF*) (Fig. 5 and 6). Comammox from WRB (as well as SR) are likely capable of degrading triuret in a similar manner as AOB, though a *trtB* is absent, indicating the carboxybiuret decarboxylation step may be carried out by an unidentified enzyme or happen spontaneously (31). In AOA, the potential pathways for degrading triuret or biuret are less clear (Fig. 6; Fig. S15). Although several AOA from WRB sediments harbored a *biuH* gene, the gene synteny of contigs suggests that multiple possible pathways could occur. Further biochemical studies are necessary to confirm the substrate utilized by the proposed *biuH* in AOA. However, we suggest that the BiuH enzyme likely acts on one or more of the following: triuret, carboxybiuret, and/or biuret. We suggest that the uncharacterized “*gatA*-like” amidohydrolase collocated with *biuH* may function as an allophanate hydrolase, allowing triuret/biuret/carboxybiuret to be degraded through allophanate to ammonia. Some *biuH*-contigs in AOA also encode FAH family proteins that could function in ureide degradation, and the common co-occurrence of *purE* also suggests that some other, potentially upstream purine degradation product may be further degraded by AOA themselves to become triuret/biuret/carboxybiuret. Some *biuH*-contigs also encode a cytosine permease (*codB*), indicating that pyrimidine breakdown products may also be used in these pathways.

Both comammox and AOA encoded *allFGHK* which could allow them to carry out the last steps of allantoin degradation: oxalurate degradation to oxamate and ammonia (50). The collocation of genes for both biuret and oxalurate degradation pathways in AOA and comammox suggests that these ammonia oxidizers may utilize several different purine degradation products produced by other microbial community members, as the upstream genes for allantoin/purine degradation were absent from nitrifier MAGs. It has recently been proposed that purine and pyrimidine cross-feeding is common in the global oceans between abundant community members SAR11, *Prochlorococcus*, and AOA (23); perhaps purine metabolic handoffs (68) are occurring in the WRB.

Despite metabolic versatility to use several organic N sources, nitrifiers in WRB lack the genetic potential to degrade guanidine, as recently described for some comammox and potentially AOB (29). However, several AOA harbor *atzF* functioning in an unknown pathway. It is possible that AOA produce allophanate from some purine- or pyrimidine-related degradation process; alternatively, allophanate could be produced by other community members and then taken up and degraded by AOA. The *atzF* gene appears to be rare in AOA genomes overall (Fig. 2), and physiological and biochemical studies are required to confirm whether *atzF* in AOA acts on allophanate as a substrate.

Dynamic floodplain environment may select for nitrifiers utilizing organic N compounds

Although aerobic ammonia oxidizers generally have high substrate affinity for ammonia, this affinity varies between different guilds (i.e., AOB versus AOA versus comammox [69, 70]) and lineages (i.e., marine versus terrestrial AOA [71]). This variability in substrate affinity is thought to play a key role in the competition between and niche partitioning of AOA, AOB, and comammox in the environment (72–76). Not only do aerobic ammonia oxidizer guilds have different affinities for ammonia but also different preferences for utilizing ammonia versus other N substrates when available. In culture-based experiments, both AOA and comammox preferred to utilize ammonia over urea and switched to urea utilization only when ammonia was depleted (27). In contrast, cultured AOB from the *Betaproteobacteria* (i.e., *Nitrosomonas* and *Nitrosospira*) preferentially utilized urea over ammonia, and AOB from the *Gammaproteobacteria* (i.e., *Nitrosococcus*) utilized both urea and ammonia when both substrates were available (27). Preferences for different N sources when multiple are available could allow for co-existence of nitrifiers in different conditions. For example, urea fertilization allows for the co-occurrence of comammox, AOB, and NOB in continuous flow reactors (25), as well as AOA and AOB in soil microcosms (26) and subsurface aquifer sediments (77). In addition to urea, the availability of the substrate cyanate could also impact nitrifier competition, co-occurrence, and niche partitioning. Cyanate can serve as the sole energy and N source for *Nitrososphaera gargensis* in culture (18) and can be used for reciprocal feeding between AOA and NOB (17, 18). How substrate preferences for urea, cyanate, or other organic N compounds impact nitrifier activity and niche partitioning in highly fluctuating environments has yet to be fully explored.

In this study, most nitrifiers in the non-redundant MAG data set (59%) encoded urea transport and urease genes. Not only does urea appear to be of potential importance to all four guilds of nitrifiers, but *cynS* was also encoded in many (24%) of these MAGs, including in comammox, NOB, and AOA. Cyanase is not commonly found in AOA genomes (47) and has been reported in *Nitrososphaera garagensis* (18) and previously generated MAGs from the WRB (13); however, cyanate can be both an energy and nitrogen source for AOA in ocean waters of the Gulf of Mexico and *Nitrosopumilus maritimus* cultures, despite the absence of canonical *cynS* (17). In addition to cyanate, the presence of putative *nit1*, *nit2*, and *nthA* in AOA and *nit1* in AOB supports the idea that some nitriles or dicarboxylic acid monamides may also support ammonia oxidation in the WRB. However, the substrates used by these enzymes have not been experimentally verified in nitrifiers, nor has their role in supplying N been confirmed. And as discussed in detail above, proposed degradation pathways for triuret, biuret, oxalurate, and allophanate were present in ammonia oxidizer MAGs in the WRB. The robust presence of genes encoding for organic N utilization raises several questions, including: why might these genes be prevalent in WRB MAGs, and what are the potential sources of organic N in the WRB floodplain?

Floodplains can receive nutrients from multiple sources, including from pulses of stream-derived allochthonous material (e.g., sediments, organic matter), atmospheric deposition, autochthonous organic matter (e.g., leaf litter), and groundwater (78, 79), which is influenced by subsurface exchanges between terrestrial and riverine systems, precipitation, and anthropogenic inputs. Generally, floodplain flow and flood pulses (80) stimulate the release of nutrients from decaying organic matter and previously deposited sediments (81–83). After the snowmelt-driven flow/flood pulse in spring, the WRB experiences summer drought conditions (12) that could decrease the rates of ammonification (39, 84). Although ammonia measurements from the WRB are lacking, the numeric predominance of AOA suggests a low ammonia supply in the floodplain. If ammonification from other microbial community members decreases under dry conditions, nitrifiers may directly degrade organic N compounds to supply ammonia. Net N-mineralization rates can remain unchanged despite differences in ammonification and nitrification rates in floodplain environments (84), perhaps related to nitrifier degradation of organic N compounds.

The WRB floodplain is densely vegetated with steppe flora, such as sagebrush, grasses, and willows, which may act as key sources of organic N outside of the rapid release of nutrients during flooding. Snowmelt-driven inundation, strong evapotranspiration (85), and high sulfate concentrations could all lead to plant stress and production of organic N compounds, particularly allantoin, that supply N to the sediment microbial community. Allantoin is an abundant N compound in plants that accumulates during drought and salinity stress (86, 87) and can also serve as a vital and sole N source for microorganisms (50, 88, 89). Allantoin can be catabolized via several different pathways that generate not only urea but also oxalurate (50). It is possible that plants also generate triuret as a side product during stress and defense responses that produce both uric acid and reactive oxygen species (31–33, 88). Additionally, nitriles may be produced by plants as cyanogenic glycosides and glucosinolates during pathogen defense (64).

In addition to live plants, buried organic matter or microbially produced dissolved organic matter (DOM) could supply organic N. For example, as key components of DNA, RNA, and some coenzymes, purines are released as organic matter is remineralized or during microbial cell lysis. Purines can also be excreted by active microbial communities (90, 91). Additionally, cyanate is found in low abundance but is rapidly cycled in terrestrial environments (92), perhaps originating from organic matter degradation as observed in the ocean. In estuarine and marine environments, a major proposed cyanate source is the photochemical degradation of DOM (93–95), specifically polypeptides and aromatic compounds (95). Cyanate can also form from the non-enzymatic decomposition of the nucleotide precursor/degradation product carbamoyl phosphate (96, 97).

In the WRB, organic N could also originate from upstream or neighboring agricultural activities and include sources, such as herbicides, livestock manure, and fertilizers. Symmetrical (s)-triazines are a suite of anthropogenic compounds, including herbicides, that generally break down to cyanuric acid which can then be degraded into biuret and allophanate (53, 54, 98). Although we did not find cyanuric acid hydrolase (*atzD*) genes in any WRB nitrifier MAGs, other microbes could supply biuret from this pathway to them. Nearby or past livestock grazing could be a source of purines and pyrimidines in floodplain sediments. Livestock manure and fertilizer runoff are common sources of organic N in freshwater systems (99). Decomposing manure produces purines and pyrimidines, impacting microbial carbon and N-cycling in soils and sediments (100–103). Urea-based fertilizer can supply not only urea but also triuret and biuret, which are by-products of urea pyrolysis, and even cyanate, as it can form from the spontaneous urea dissociation in an aqueous solution (104, 105). Nitriles in the terrestrial environment can also come from anthropogenic sources, such as from acrylamide, pharmaceuticals, herbicides, mining, metallurgical processes, wastewater discharge, and fuel combustion (106). Our WRB site is near some human development (Riverton, WY) and is a DOE legacy site due to persistent groundwater contamination from past uranium and vanadium ore processing (107), making other anthropogenic sources of nitriles possible. The presence of human development has shown a clear impact on DOM composition in rivers (108); thus, it is possible that several different anthropogenically-derived organic N compounds could be present in the river and groundwater. Further research could elucidate whether such compounds are present and whether they correlate with the organic N utilization genes described here.

It has been hypothesized that the introduction of s-triazine herbicides has led to the evolution of the enzyme 1-carboxybiuret hydrolase *atzEG* from the *gatA* and *gatC* of the glutamyl-tRNA amidotransferase and that indirect tRNA aminoacylation can be a source of alternative functions (109). The uncharacterized *gatA*-like amidohydrolase found collocated with *biuH* in some AOA MAGs may be an example of an alternative function originating from genes involved in tRNA aminoacylations. In further support of this, these uncharacterized *gatA*-like amidohydrolases are present in lineages of the *Nitrososphaeraceae* (Fig. 4), which phylogenomic analysis and ancestral state reconstruction suggest has undergone a high level of proteome expansion through gene duplication and loss (59). The origination of novel functions could enable some *Nitrososphaeraceae* lineages found in the WRB to utilize additional organic compounds as N sources and thrive in dynamic, and perhaps contaminated, floodplain environments. Physiological studies are necessary to confirm the substrates utilized in the proposed purine degradation pathways described in this study, as well as putative nitrilases/omega amidases annotated in nitrifier MAGs. Additionally, metatranscriptomic or metaproteomic studies would illuminate if and under what conditions the proposed pathways for utilizing organic N are active, and whether nitrifier lineages utilize different substrates *in situ*. The presence of putative novel pathways related to purine degradation, as well as for cyanate and nitrile degradation, in nitrifier genomes suggests both the presence of diverse organic N compounds in WRB sediments that warrant characterization and a potentially large role for nitrifiers in net N mineralization.

Conclusions

Diverse AOA MAGs were recovered from WRB floodplain sediments. Our findings add additional AOA lineages to those reported in Reji et al. (13), as well as highlight the diversity and genetic potential of AOB, comammox, and NOB MAGs present in floodplain sediments. We observed taxonomically diverse and depth-differentiated nitrifier populations with marine-like lineages residing in deeper depths. Several different mechanisms for utilizing organic N sources are present in MAGs and include genes related to utilizing cyanate, nitriles, and glutamine, as well as purine degradation products, such as urea, triuret, biuret, oxalurate, and allophanate. This study increases our understanding of the possible N substrates supporting nitrification and suggests that dynamic floodplains can select for metabolically versatile nitrifiers. Given the presence of *biuH* and *allFGHK* in a cultured representative of AOA (*Nitrososphaera viennensis* [58]) and an enriched comammox (*Ca*. Nitrospira nitrificans [51]), future laboratory studies utilizing different substrates to supply N would yield great insights into the proposed pathways and substrates used by the enzymes identified in this study.

MATERIALS AND METHODS

Field sample collection

Floodplain sediments in the WRB were sampled for microbial community analysis near Riverton, WY, USA, at three nearby sites across three field seasons (2015, 2017, and 2019) (Fig. 1). In 2015, samples were collected in August at site KB1 (42.98871, −108.39963) from 0 to 234 cm below ground surface (detailed sampling methods and sediment characteristics available in [11, 13]). In 2017, samples were collected in May, twice in July, and September at site Pit2 (42.98864, −108.40006) from 10 to ~150 cm (detailed sampling methods and sediment characteristics available in [12] and associated geochemical data in [110]). In 2019, samples were collected at site PTT1 (42.98831, −108.40036) in June, August, and October from 60 to 180 cm. All three sites are located on an alluvial terrace near the confluence of the Wind River and Little Wind River with varying distance (50 to 100 m) from the Little Wind River main channel (Fig. 1). Sampling depths include dry, unsaturated sediments to transiently wet and saturated depths (Fig. 1). In general, sediment samples for microbial analyses were collected at discrete depths at ~10–30 cm intervals (depending on soil horizonation, sampling year, and location) along the length of the core, flash-frozen in liquid nitrogen or on dry ice, and stored at −80°C until nucleic acid extraction.

Metagenome and MAG processing

DNA extraction methods are available in the Supplemental Materials and Methods. A total of 68 DNA samples were submitted to and sequenced by the DOE Joint Genome Institute (JGI) either via a FICUS project (Proposal ID: 504298) or a CSP Project (Proposal ID: 1927). Quality-controlled filtered raw metagenome data (accessions available in Table S2) were downloaded from the JGI Genome Portal for assembly, binning, and refining using the metaWRAP (v1.3.2) pipeline (111). Assemblies were made using MEGAHIT (v1.3.3). Samples from 2019 were also co-assembled by depth. All assemblies were binned using contigs >2,000 nt with MetaBAT2 (v2.12.1) (112) and MaxBin 2.0 (v2.2.6) (113). Single sample assemblies from 2017 were also binned using multiple fastq files and additionally using CONCOCT (v1.0.0) (114). All bins generated from a given metagenome were consolidated and filtered using *metawrap bin_refinement* and then further refined with MAGpurify (v1.0) (115). Any MAGs with >50% completeness and >10% redundancy were manually refined using anvi'o (v8) (116) *anvi-refine* and *anvi-summarize*. MAGs were retained if they were determined to be above >50% completeness and have <10% contamination as calculated via CheckM (v1.1.3) (117). All MAGs were dereplicated using dRep (v3.1.1) (118) at 98% ANI to create a non-redundant MAG data set, and we refer to these representative MAGs as lineages. Taxonomic classification for each representative MAG was made using the GTDB toolkit (GTDB-tk, v2.4.0) (119) with the database release RS220. Reads were competitively recruited to non-redundant MAG data set using Bowtie2 (v2.4.2) (120) with default parameters. Coverage values and read alignment rates per genome were calculated using CoverM (v0.4.0) (121). Abundances are displayed as unpaired reads recruited per genome size of MAG in kilobases of MAG, divided by gigabases of metagenome (RPKG). Genes were called and translated using Prodigal (v2.6.3), and annotations were performed via KEGG (122, 123) using GhostKOALA (v3.1) (124) and eggnog-mapper (v2.1.12) with the eggnog 5 database (125, 126). Code used in this workflow is available on GitHub (https://github.com/anna-rasmussen/MAG-analysis).

Phylogenetic analysis

Protein-protein BLAST (*blastp*) was used to query WRB MAGs and GTDB species representative genomes for genes of interest, or genes were selected from WRB and SR MAGs based on KEGG (122, 123) annotation. SR nitrifier MAGs were downloaded from PRJNA1142551 and ER from reference 127. Reference protein sequences were identified via *blastp* searches against the PDB, uniprot, refseq select, and nr databases using default parameters or by searching by gene name in PDB. Gene synteny of *biuH* and *atzF* contigs across different genomes was generated and visualized using SimpleSynteny (v1.6b) (128) with a significance value of 0.001 and 50% alignment length. If multiple genes were mapped to a given gene, the one with the highest bit score was kept. Gene sequence alignments were carried out using Clustal Omega (v1.2.3) (129), and the ends were manually trimmed in Geneious Prime (v2024.0.7). Concatenated ribosomal alignments were created using anvi'o with *anvi-get-sequences-for-hmm-hits*, aligned using MUSCLE (v3.8.1551) (130), and trimmed using trimAl (v1.4.rev15). All phylogenetic trees were constructed using IQ-TREE2 (v2.0.3) (131) with ModelFinder *-MFP* (132) to identify the best fit model and 1,000 bootstraps. Phylogenetic trees were visualized using FigTree (v1.4.4) (133) and iTOL (v6) (134). Nucleotide AOA *amoA* sequences were aligned with the updated alignment in (45) based on the unified definitions established in Alves et al. (42) for classification.

ACKNOWLEDGMENTS

This work was supported by the Watershed Function Science Focus Area at SLAC Accelerator Laboratory funded by the US Department of Energy, Office of Science, Biological and Environmental Research under Contract No. DE-AC02-76SF00515 and by contract DE-SC0019119 to C.A.F. We gratefully acknowledge substantial logistical support from the US Department of Energy, Office of Legacy Management, which provided access to the Riverton field site, obtained permits for operations, provided ES&H support, and conducted drilling operations. Sequencing was carried out as part of a Community Science Program (CSP) grant to C.A.F. (Proposal ID 1927) and Facilities Integrating Collaborations for User Science (FICUS) grant to K.B., B.B.T., and C.A.F. (Proposal ID 504298) from the DOE Joint Genome Institute, a DOE Office of Science User Facility supported by the Office of Science of the U.S. Department of Energy under Contract No. DE-AC02-05CH11231; special thanks to C. Pennacchio for JGI support. Some of the computing for this project was performed on the Sherlock cluster. We would like to thank Stanford University and the Stanford Research Computing Center for providing computational resources and support that contributed to these research results. We thank the Northern Arapaho Natural Resources Office and St. Stephens Indian Mission for field access and support, especially R. Ortiz, S. Babits, and D. Goggles. Additional support was provided by the DOE office of Legacy Management (LM) and Navarro Research and Engineering, Inc., especially W. Frazier, S. Campbell, and R. L. Johnson. We thank L. Spielman, A. Ederer, and S-M. Kilpatrick for sample processing for this project, with support from the Stanford Earth Summer Undergraduate Research (SESUR) and Stanford's Summer Undergraduate Research in Geoscience and Engineering (SURGE) Programs. Thank you to B. Shapero for input on protein analysis.

AUTHOR AFFILIATIONS

[1]Stanford Synchrotron Radiation Lightsource, SLAC National Accelerator Laboratory, Menlo Park, California, USA
[2]Department of Earth System Science, Stanford University, Stanford, California, USA
[3]Environmental Molecular Sciences Laboratory, Pacific Northwest National Laboratory, Richland, Washington, USA
[4]Oceans Department, Stanford University, Stanford, California, USA

PRESENT ADDRESS

Katie Langenfeld, Department of Ecology and Evolutionary Biology, University of Michigan, Ann Arbor, Michigan, USA
Bradley B. Tolar, Department of Biology and Marine Biology, University of North Carolina Wilmington, Wilmington, North Carolina, USA
Zach Perzan, Department of Geoscience, University of Nevada Las Vegas, Las Vegas, Nevada, USA
Emily L. Cardarelli, Department of Earth, Planetary, and Space Sciences, University of California Los Angeles, Los Angeles, California, USA

AUTHOR ORCIDs

Anna N. Rasmussen http://orcid.org/0000-0002-0031-2835
Katie Langenfeld http://orcid.org/0000-0002-2741-2254
Bradley B. Tolar http://orcid.org/0000-0003-0493-1470
Christopher A. Francis http://orcid.org/0000-0001-7557-631X

FUNDING

Funder	Grant(s)	Author(s)
U.S. Department of Energy	DE-SC0019119	Christopher A. Francis
U.S. Department of Energy	DE-AC02-76SF00515	John R. Bargar

AUTHOR CONTRIBUTIONS

Anna N. Rasmussen, Data curation, Formal analysis, Investigation, Methodology, Software, Visualization, Writing – original draft, Writing – review and editing | Katie Langenfeld, Data curation, Methodology, Software, Writing – review and editing | Bradley B. Tolar, Data curation, Funding acquisition, Investigation, Methodology, Resources, Writing – review and editing | Zach Perzan, Data curation, Investigation, Methodology, Resources, Writing – review and editing | Kate Maher, Conceptualization, Funding acquisition, Supervision, Writing – review and editing | Emily L. Cardarelli, Conceptualization, Data curation, Funding acquisition, Investigation, Methodology, Resources, Writing – review and editing | John R. Bargar, Conceptualization, Funding acquisition, Investigation, Methodology, Project administration, Resources, Supervision | Kristin Boye, Conceptualization, Funding acquisition, Investigation, Resources, Supervision, Writing – review and editing | Christopher A. Francis, Conceptualization, Funding acquisition, Supervision, Writing – review and editing

DATA AVAILABILITY

The 68 metagenomes used in this study are available in both NCBI and IMG (JGI) databases, with accession numbers provided in Table S2. All metagenomes can be found under GOLD study IDs Gs0142591 (2017) and Gs0131241 (2015, 2019). All MAGs generated in this study along with quality metrics, GTDB taxonomy, and metagenome of origin accessions are available in the ESS-DIVE data repository under doi:10.15485/2563565 (135), doi:10.15485/2563574 (136), and doi:10.15485/2563566 (137). Nitrifier MAG quality is also available in Table S1.

ADDITIONAL FILES

The following material is available online.

Supplemental Material

Supplemental file (mSystems00829-25-s0001.pdf). Supplemental text and Fig. S1-S21.
Table S1 (mSystems00829-25-s0002.csv). GTDB RS220 taxonomy, MAG quality metrics, and metagenome accession numbers for nitrifier MAGs.
Table S2 (mSystems00829-25-s0003.csv). Metagenome accession numbers for floodplain sediment samples assembled and binned.

REFERENCES

1. Vidon P, Allan C, Burns D, Duval TP, Gurwick N, Inamdar S, Lowrance R, Okay J, Scott D, Sebestyen S. 2010. Hot spots and hot moments in riparian zones: potential for improved water quality management[1]. J American Water Resour Assoc 46:278–298. https://doi.org/10.1111/j.1752-1688.2010.00420.x
2. Noël V, Boye K, Kukkadapu RK, Bone S, Lezama Pacheco JS, Cardarelli E, Janot N, Fendorf S, Williams KH, Bargar JR. 2017. Understanding controls on redox processes in floodplain sediments of the Upper Colorado River Basin. Sci Total Environ 603–604:663–675. https://doi.org/10.1016/j.scitotenv.2017.01.109
3. Noël V, Boye K, Kukkadapu RK, Li Q, Bargar JR. 2019. Uranium storage mechanisms in wet-dry redox cycled sediments. Water Res 152:251–263. https://doi.org/10.1016/j.watres.2018.12.040
4. Noël V, Boye K, Lezama Pacheco JS, Bone SE, Janot N, Cardarelli E, Williams KH, Bargar JR. 2017. Redox controls over the stability of U(IV) in floodplains of the upper Colorado River Basin. Environ Sci Technol 51:10954–10964. https://doi.org/10.1021/acs.est.7b02203
5. McClain ME, Boyer EW, Dent CL, Gergel SE, Grimm NB, Groffman PM, Hart SC, Harvey JW, Johnston CA, Mayorga E, McDowell WH, Pinay G. 2003. Biogeochemical hot spots and hot moments at the interface of terrestrial and aquatic ecosystems. Ecosystems (N Y, Print) 6:301–312. https://doi.org/10.1007/s10021-003-0161-9
6. Dwivedi D, Arora B, Steefel CI, Dafflon B, Versteeg R. 2018. Hot spots and hot moments of nitrogen in a riparian corridor. Water Resour Res 54:205–222. https://doi.org/10.1002/2017WR022346
7. Boano F, Harvey JW, Marion A, Packman AI, Revelli R, Ridolfi L, Wörman A. 2014. Hyporheic flow and transport processes: mechanisms, models, and biogeochemical implications. Rev Geophys 52:603–679. https://doi.org/10.1002/2012RG000417
8. Vitousek PM, Aber JD, Howarth RW, Likens GE, Matson PA, Schindler DW, Schlesinger WH, Tilman DG. 1997. Human alteration of the global nitrogen cycle: sources and consequences. Ecol Appl 7:737–750. https://doi.org/10.1890/1051-0761(1997)007[0737:HAOTGN]2.0.CO;2
9. Matheus Carnevali PB, Lavy A, Thomas AD, Crits-Christoph A, Diamond S, Méheust R, Olm MR, Sharrar A, Lei S, Dong W, Falco N, Bouskill N, Newcomer ME, Nico P, Wainwright H, Dwivedi D, Williams KH, Hubbard S, Banfield JF. 2021. Meanders as a scaling motif for understanding of floodplain soil microbiome and biogeochemical potential at the watershed scale. Microbiome 9:121. https://doi.org/10.1186/s40168-020-00957-z
10. Rasmussen AN, Tolar BB, Bargar JR, Boye K, Francis CA. 2025. Metagenome-assembled genomes for oligotrophic nitrifiers from a mountainous gravelbed floodplain. Environ Microbiol 27:e70060. https://doi.org/10.1111/1462-2920.70060
11. Cardarelli EL, Bargar JR, Francis CA. 2020. Diverse *Thaumarchaeota* dominate subsurface ammonia-oxidizing communities in semi-arid

floodplains in the Western United States. Microb Ecol 80:778–792. https://doi.org/10.1007/s00248-020-01534-5
12. Tolar BB, Boye K, Bobb C, Maher K, Bargar JR, Francis CA. 2020. Stability of floodplain subsurface microbial communities through seasonal hydrological and geochemical cycles. Front Earth Sci 8:338. https://doi.org/10.3389/feart.2020.00338
13. Reji L, Cardarelli EL, Boye K, Bargar JR, Francis CA. 2022. Diverse ecophysiological adaptations of subsurface Thaumarchaeota in floodplain sediments revealed through genome-resolved metagenomics. ISME J 16:1140–1152. https://doi.org/10.1038/s41396-021-01167-7
14. Bento M de S, Barros DJ, Araújo MG da S, Da Róz R, Carvalho GA, do Carmo JB, Toppa RH, Neu V, Forsberg BR, Bodelier PLE, Tsai SM, Navarrete AA. 2021. Active methane processing microbes and the disproportionate role of NC10 phylum in methane mitigation in Amazonian floodplains. Biogeochemistry 156:293–317. https://doi.org/10.1007/s10533-021-00846-z
15. Gontijo JB, Paula FS, Venturini AM, Yoshiura CA, Borges CD, Moura JMS, Bohannan BJM, Nüsslein K, Rodrigues JLM, Tsai SM. 2021. Not just a methane source: Amazonian floodplain sediments harbour a high diversity of methanotrophs with different metabolic capabilities. Mol Ecol 30:2560–2572. https://doi.org/10.1111/mec.15912
16. Monteiro GGTN, Barros DJ, Gabriel GVM, Venturini AM, Veloso TGR, Vazquez GH, Oliveira LC, Neu V, Bodelier PLE, Mansano CFM, Tsai SM, Navarrete AA. 2022. Molecular evidence for stimulation of methane oxidation in Amazonian floodplains by ammonia-oxidizing communities. Front Microbiol 13:913453. https://doi.org/10.3389/fmicb.2022.913453
17. Kitzinger K, Padilla CC, Marchant HK, Hach PF, Herbold CW, Kidane AT, Könneke M, Littmann S, Mooshammer M, Niggemann J, Petrov S, Richter A, Stewart FJ, Wagner M, Kuypers MMM, Bristow LA. 2019. Cyanate and urea are substrates for nitrification by *Thaumarchaeota* in the marine environment. Nat Microbiol 4:234–243. https://doi.org/10.1038/s41564-018-0316-2
18. Palatinszky M, Herbold C, Jehmlich N, Pogoda M, Han P, von Bergen M, Lagkouvardos I, Karst SM, Galushko A, Koch H, Berry D, Daims H, Wagner M. 2015. Cyanate as an energy source for nitrifiers. Nature 524:105–108. https://doi.org/10.1038/nature14856
19. Koper TE, El-Sheikh AF, Norton JM, Klotz MG. 2004. Urease-encoding genes in ammonia-oxidizing bacteria. Appl Environ Microbiol 70:2342–2348. https://doi.org/10.1128/AEM.70.4.2342-2348.2004
20. Tolar BB, Wallsgrove NJ, Popp BN, Hollibaugh JT. 2017. Oxidation of urea-derived nitrogen by thaumarchaeota-dominated marine nitrifying communities. Environ Microbiol 19:4838–4850. https://doi.org/10.1111/1462-2920.13457
21. Kitzinger K, Marchant HK, Bristow LA, Herbold CW, Padilla CC, Kidane AT, Littmann S, Daims H, Pjevac P, Stewart FJ, Wagner M, Kuypers MMM. 2020. Single cell analyses reveal contrasting life strategies of the two main nitrifiers in the ocean. Nat Commun 11:767. https://doi.org/10.1038/s41467-020-14542-3
22. Koch H, Lücker S, Albertsen M, Kitzinger K, Herbold C, Spieck E, Nielsen PH, Wagner M, Daims H. 2015. Expanded metabolic versatility of ubiquitous nitrite-oxidizing bacteria from the genus *Nitrospira*. Proc Natl Acad Sci USA 112:11371–11376. https://doi.org/10.1073/pnas.1506533112
23. Braakman R, Satinsky B, O'Keefe TJ, Longnecker K, Hogle SL, Becker JW, Li RC, Dooley K, Arellano A, Kido Soule MC, Kujawinski EB, Chisholm SW. 2025. Global niche partitioning of purine and pyrimidine cross-feeding among ocean microbes. Sci Adv 11:eadp1949. https://doi.org/10.1126/sciadv.adp1949
24. Damashek J, Tolar BB, Liu Q, Okotie‐Oyekan AO, Wallsgrove NJ, Popp BN, Hollibaugh JT. 2019. Microbial oxidation of nitrogen supplied as selected organic nitrogen compounds in the South Atlantic Bight. Limnol Oceanogr 64:982–995. https://doi.org/10.1002/lno.11089
25. Vilardi KJ, Johnston J, Dai Z, Cotto I, Tuttle E, Patterson A, Stubbins A, Pieper KJ, Pinto AJ. 2024. Nitrogen source influences the interactions of comammox bacteria with aerobic nitrifiers. Microbiol Spectr 12:e0318123. https://doi.org/10.1128/spectrum.03181-23
26. Hink L, Gubry-Rangin C, Nicol GW, Prosser JI. 2018. The consequences of niche and physiological differentiation of archaeal and bacterial ammonia oxidisers for nitrous oxide emissions. ISME J 12:1084–1093. https://doi.org/10.1038/s41396-017-0025-5
27. Qin W, Wei SP, Zheng Y, Choi E, Li X, Johnston J, Wan X, Abrahamson B, Flinkstrom Z, Wang B, et al. 2024. Ammonia-oxidizing bacteria and archaea exhibit differential nitrogen source preferences. Nat Microbiol 9:524–536. https://doi.org/10.1038/s41564-023-01593-7
28. Liu Q, Chen Y, Xu X-W. 2023. Genomic insight into strategy, interaction and evolution of nitrifiers in metabolizing key labile-dissolved organic nitrogen in different environmental niches. Front Microbiol 14. https://doi.org/10.3389/fmicb.2023.1273211
29. Palatinszky M, Herbold CW, Sedlacek CJ, Pühringer D, Kitzinger K, Giguere AT, Wasmund K, Nielsen PH, Dueholm MKD, Jehmlich N, Gruseck R, Legin A, Kostan J, Krasnici N, Schreiner C, Palmetzhofer J, Hofmann T, Zumstein M, Djinović-Carugo K, Daims H, Wagner M. 2024. Growth of complete ammonia oxidizers on guanidine. Nature 633:646–653. https://doi.org/10.1038/s41586-024-07832-z
30. Kerou M, Ponce-Toledo RI, Zhao R, Abby SS, Hirai M, Nomaki H, Takaki Y, Nunoura T, Jørgensen SL, Schleper C. 2021. Genomes of Thaumarchaeota from deep sea sediments reveal specific adaptations of three independently evolved lineages. ISME J 15:2792–2808. https://doi.org/10.1038/s41396-021-00962-6
31. Tassoulas LJ, Elias MH, Wackett LP. 2021. Discovery of an ultraspecific triuret hydrolase (TrtA) establishes the triuret biodegradation pathway. J Biol Chem 296:100055. https://doi.org/10.1074/jbc.RA120.015631
32. Gersch C, Palii SP, Imaram W, Kim KM, Karumanchi SA, Angerhofer A, Johnson RJ, Henderson GN. 2009. Reactions of peroxynitrite with uric acid: formation of reactive intermediates, alkylated products and triuret, and *in vivo* production of triuret under conditions of oxidative stress. Nucleosides Nucleotides Nucleic Acids 28:118–149. https://doi.org/10.1080/15257770902736400
33. Robinson KM, Morré JT, Beckman JS. 2004. Triuret: a novel product of peroxynitrite-mediated oxidation of urate. Arch Biochem Biophys 423:213–217. https://doi.org/10.1016/j.abb.2003.10.011
34. GriffinJL. 1960. The isolation, characterization, and identification of the crystalline inclusions of the large free-living amebae. J Biophys Biochem Cytol 7:227–234. https://doi.org/10.1083/jcb.7.2.227
35. Cerecedo LR. 1933. The chemistry and metabolism of the nucleic acids, purines, and Pyrimidines. Annu Rev Biochem 2:109–128. https://doi.org/10.1146/annurev.bi.02.070133.000545
36. Low AJ, Piper FJ. 1970. The ammonification and nitrification in soil of urea with and without biuret. J Agric Sci 75:301–309. https://doi.org/10.1017/S0021859600016993
37. Xue J, Clinton PW, Sands R, Payn TW. 2022. Mineralisation and nitrification of biuret and urea nitrogen in two New Zealand forest soils. Soil Res 61:37–46. https://doi.org/10.1071/SR21243
38. Hays JT, Hewson WB. 1973. Controlled release fertilizers by chemical modification of urea. Triuret. J Agric Food Chem 21:498–499. https://doi.org/10.1021/jf60187a031
39. Wolf KL, Noe GB, Ahn C. 2013. Hydrologic connectivity to streams increases nitrogen and phosphorus inputs and cycling in soils of created and natural floodplain wetlands. J Environ Qual 42:1245–1255. https://doi.org/10.2134/jeq2012.0466
40. Yabusaki SB, Wilkins MJ, Fang Y, Williams KH, Arora B, Bargar J, Beller HR, Bouskill NJ, Brodie EL, Christensen JN, Conrad ME, Danczak RE, King E, Soltanian MR, Spycher NF, Steefel CI, Tokunaga TK, Versteeg R, Waichler SR, Wainwright HM. 2017. Water table dynamics and biogeochemical cycling in a shallow, variably-saturated floodplain. Environ Sci Technol 51:3307–3317. https://doi.org/10.1021/acs.est.6b04873
41. Bouskill NJ, Conrad ME, Bill M, Brodie EL, Cheng Y, Hobson C, Forbes M, Casciotti KL, Williams KH. 2019. Evidence for microbial mediated NO_3^- cycling within floodplain sediments during groundwater fluctuations. Front Earth Sci 7. https://doi.org/10.3389/feart.2019.00189
42. Alves RJE, Minh BQ, Urich T, von Haeseler A, Schleper C. 2018. Unifying the global phylogeny and environmental distribution of ammonia-oxidising archaea based on *amoA* genes. Nat Commun 9:1517. https://doi.org/10.1038/s41467-018-03861-1
43. Offre P, Kerou M, Spang A, Schleper C. 2014. Variability of the transporter gene complement in ammonia-oxidizing archaea. Trends Microbiol 22:665–675. https://doi.org/10.1016/j.tim.2014.07.007
44. Nakagawa T, Stahl DA. 2013. Transcriptional response of the archaeal ammonia oxidizer *Nitrosopumilus maritimus* to low and environmentally relevant ammonia concentrations. Appl Environ Microbiol 79:6911–6916. https://doi.org/10.1128/AEM.02028-13
45. Redondo MA, Jones CM, Legendre P, Guénard G, Hallin S. 2025. Predicting gene distribution in ammonia-oxidizing archaea using phylogenetic signals. ISME Commun 5:ycaf087. https://doi.org/10.1093/ismeco/ycaf087

46. Qin W, Zheng Y, Zhao F, Wang Y, Urakawa H, Martens-Habbena W, Liu H, Huang X, Zhang X, Nakagawa T, et al. 2020. Alternative strategies of nutrient acquisition and energy conservation map to the biogeography of marine ammonia-oxidizing archaea. ISME J 14:2595–2609. https://doi.org/10.1038/s41396-020-0710-7
47. Wright CL, Lehtovirta-Morley LE. 2023. Nitrification and beyond: metabolic versatility of ammonia oxidising archaea. ISME J 17:1358–1368. https://doi.org/10.1038/s41396-023-01467-0
48. Kim NY, Kim OB. 2024. Oxamic transcarbamylase of *Escherichia coli* is encoded by the three genes *allFGH* (formerly *fdrA*, *ylbE*, and *ylbF*). Appl Environ Microbiol 90:e00957-24. https://doi.org/10.1128/aem.00957-24
49. Kim NY, Kim OB. 2022. The *ybcF* gene of *Escherichia coli* encodes a local orphan enzyme, catabolic carbamate kinase. J Microbiol Biotechnol 32:1527–1536. https://doi.org/10.4014/jmb.2210.10037
50. Huynh TN, Stewart V. 2023. Purine catabolism by enterobacteria. Adv Microb Physiol 82:205–266. https://doi.org/10.1016/bs.ampbs.2023.01.001
51. van Kessel M, Speth DR, Albertsen M, Nielsen PH, Op den Camp HJM, Kartal B, Jetten MSM, Lücker S. 2015. Complete nitrification by a single microorganism. Nature 528:555–559. https://doi.org/10.1038/nature16459
52. Tassoulas LJ, Robinson A, Martinez-Vaz B, Aukema KG, Wackett LP. 2021. Filling in the gaps in metformin biodegradation: a new enzyme and a metabolic pathway for guanylurea. Appl Environ Microbiol 87:e03003-20. https://doi.org/10.1128/AEM.03003-20
53. Robinson SL, Badalamenti JP, Dodge AG, Tassoulas LJ, Wackett LP. 2018. Microbial biodegradation of biuret: defining biuret hydrolases within the isochorismatase superfamily. Environ Microbiol 20:2099–2111. https://doi.org/10.1111/1462-2920.14094
54. Aukema KG, Tassoulas LJ, Robinson SL, Konopatski JF, Bygd MD, Wackett LP. 2020. Cyanuric acid biodegradation via biuret: physiology, taxonomy, and geospatial distribution. Appl Environ Microbiol 86:e01964-19. https://doi.org/10.1128/AEM.01964-19
55. Esquirol L, Peat TS, Wilding M, Lucent D, French NG, Hartley CJ, Newman J, Scott C. 2018. Structural and biochemical characterization of the biuret hydrolase (BiuH) from the cyanuric acid catabolism pathway of *Rhizobium leguminasorum* bv. *viciae* 3841. PLoS One 13:e0192736. https://doi.org/10.1371/journal.pone.0192736
56. Tumbula DL, Becker HD, Chang WZ, Söll D. 2000. Domain-specific recruitment of amide amino acids for protein synthesis. Nature 407:106–110. https://doi.org/10.1038/35024120
57. Weiss AKH, Loeffler JR, Liedl KR, Gstach H, Jansen-Dürr P. 2018. The fumarylacetoacetate hydrolase (FAH) superfamily of enzymes: multifunctional enzymes from microbes to mitochondria. Biochem Soc Trans 46:295–309. https://doi.org/10.1042/BST20170518
58. Stieglmeier M, Klingl A, Alves RJE, Rittmann SK-MR, Melcher M, Leisch N, Schleper C. 2014. *Nitrososphaera viennensis* gen. nov., sp. nov., an aerobic and mesophilic, ammonia-oxidizing archaeon from soil and a member of the archaeal phylum *Thaumarchaeota*. Int J Syst Evol Microbiol 64:2738–2752. https://doi.org/10.1099/ijs.0.063172-0
59. Sheridan PO, Raguideau S, Quince C, Holden J, Zhang L, Williams TA, Gubry-Rangin C, Thames Consortium. 2020. Gene duplication drives genome expansion in a major lineage of Thaumarchaeota. Nat Commun 11:5494. https://doi.org/10.1038/s41467-020-19132-x
60. Daims H, Lücker S, Wagner M. 2016. A new perspective on microbes formerly known as nitrite-oxidizing bacteria. Trends Microbiol 24:699–712. https://doi.org/10.1016/j.tim.2016.05.004
61. Ngugi DK, Blom J, Stepanauskas R, Stingl U. 2016. Diversification and niche adaptations of *Nitrospina*-like bacteria in the polyextreme interfaces of Red Sea brines. ISME J 10:1383–1399. https://doi.org/10.1038/ismej.2015.214
62. Off S, Alawi M, Spieck E. 2010. Enrichment and physiological characterization of a novel *Nitrospira*-like bacterium obtained from a marine sponge. Appl Environ Microbiol 76:4640–4646. https://doi.org/10.1128/AEM.00320-10
63. Sultana R, Johnson RH, Tigar AD, Wahl TJ, Meurer CE, Hoss KN, Xu S, Paradis CJ. 2024. Contaminant mobilization from the vadose zone to groundwater during experimental river flooding events. J Contam Hydrol 265:104391. https://doi.org/10.1016/j.jconhyd.2024.104391
64. U.S. Department of Energy. 2018. 2017 Verification Monitoring Report, Riverton, Wyoming, Processing Site
65. Alonso-Sáez L, Waller AS, Mende DR, Bakker K, Farnelid H, Yager PL, Lovejoy C, Tremblay J-É, Potvin M, Heinrich F, Estrada M, Riemann L, Bork P, Pedrós-Alió C, Bertilsson S. 2012. Role for urea in nitrification by polar marine Archaea. Proc Natl Acad Sci USA 109:17989–17994. https://doi.org/10.1073/pnas.1201914109
66. Vogels GD, Van der Drift C. 1976. Degradation of purines and pyrimidines by microorganisms. Bacteriol Rev 40:403–468. https://doi.org/10.1128/br.40.2.403-468.1976
67. Werner AK, Witte C-P. 2011. The biochemistry of nitrogen mobilization: purine ring catabolism. Trends Plant Sci 16:381–387. https://doi.org/10.1016/j.tplants.2011.03.012
68. Hug LA, Co R. 2018. It takes a village: microbial communities thrive through interactions and metabolic handoffs. mSystems 3:e00152-17. https://doi.org/10.1128/mSystems.00152-17
69. Martens-Habbena W, Berube PM, Urakawa H, de la Torre JR, Stahl DA. 2009. Ammonia oxidation kinetics determine niche separation of nitrifying Archaea and Bacteria. Nature 461:976–979. https://doi.org/10.1038/nature08465
70. Kits KD, Sedlacek CJ, Lebedeva EV, Han P, Bulaev A, Pjevac P, Daebeler A, Romano S, Albertsen M, Stein LY, Daims H, Wagner M. 2017. Kinetic analysis of a complete nitrifier reveals an oligotrophic lifestyle. Nature 549:269–272. https://doi.org/10.1038/nature23679
71. Jung M-Y, Sedlacek CJ, Kits KD, Mueller AJ, Rhee S-K, Hink L, Nicol GW, Bayer B, Lehtovirta-Morley L, Wright C, de la Torre JR, Herbold CW, Pjevac P, Daims H, Wagner M. 2022. Ammonia-oxidizing archaea possess a wide range of cellular ammonia affinities. ISME J 16:272–283. https://doi.org/10.1038/s41396-021-01064-z
72. Ghimire-Kafle S, Weaver ME, Kimbrel MP, Bollmann A. 2024. Competition between ammonia-oxidizing archaea and complete ammonia oxidizers from freshwater environments. Appl Environ Microbiol 90:e0169823. https://doi.org/10.1128/aem.01698-23
73. Verhamme DT, Prosser JI, Nicol GW. 2011. Ammonia concentration determines differential growth of ammonia-oxidising archaea and bacteria in soil microcosms. ISME J 5:1067–1071. https://doi.org/10.1038/ismej.2010.191
74. Gubry-Rangin C, Nicol GW, Prosser JI. 2010. Archaea rather than bacteria control nitrification in two agricultural acidic soils. FEMS Microbiol Ecol 74:566–574. https://doi.org/10.1111/j.1574-6941.2010.00971.x
75. Tourna M, Freitag TE, Nicol GW, Prosser JI. 2008. Growth, activity and temperature responses of ammonia-oxidizing archaea and bacteria in soil microcosms. Environ Microbiol 10:1357–1364. https://doi.org/10.1111/j.1462-2920.2007.01563.x
76. Hink L, Nicol GW, Prosser JI. 2017. Archaea produce lower yields of N_2O than bacteria during aerobic ammonia oxidation in soil. Environ Microbiol 19:4829–4837. https://doi.org/10.1111/1462-2920.13282
77. Reed DW, Smith JM, Francis CA, Fujita Y. 2010. Responses of ammonia-oxidizing bacterial and archaeal populations to organic nitrogen amendments in low-nutrient groundwater. Appl Environ Microbiol 76:2517–2523. https://doi.org/10.1128/AEM.02436-09
78. Gordon BA, Dorothy O, Lenhart CF. 2020. Nutrient retention in ecologically functional floodplains: a review. Water (Basel) 12:2762. https://doi.org/10.3390/w12102762
79. Mitsch WJ, Gosselink JG. 2007. Wetlands. John Wiley & Sons.
80. Tockner K, Malard F, Ward JV. 2000. An extension of the flood pulse concept. Hydrol Process 14:2861–2883. https://doi.org/10.1002/1099-1085(200011/12)14:16/17<2861::AID-HYP124>3.0.CO;2-F
81. Naiman RJ, Décamps H. 1997. The ecology of interfaces: riparian zones. Annu Rev Ecol Syst 28:621–658. https://doi.org/10.1146/annurev.ecolsys.28.1.621
82. Xiong S, Nilsson C. 1997. Dynamics of leaf litter accumulation and its effects on riparian vegetation: a review. Bot Rev 63:240–264. https://doi.org/10.1007/BF02857951
83. Ostojić A, Rosado J, Miliša M, Morais M, Tockner K. 2013. Release of nutrients and organic matter from river floodplain habitats: simulating seasonal inundation dynamics. Wetlands (Wilmington) 33:847–859. https://doi.org/10.1007/s13157-013-0442-9
84. Noe GB, Hupp CR, Rybicki NB. 2013. Hydrogeomorphology influences soil nitrogen and phosphorus mineralization in floodplain wetlands. Ecosystems (N Y, Print) 16:75–94. https://doi.org/10.1007/s10021-012-9597-0
85. Dam WL, Campbell S, Johnson RH, Looney BB, Denham ME, Eddy-Dilek CA, Babits SJ. 2015. Refining the site conceptual model at a former uranium mill site in Riverton, Wyoming, USA. Environ Earth Sci 74:7255–7265. https://doi.org/10.1007/s12665-015-4706-y

86. Kaur H, Chowrasia S, Gaur VS, Mondal TK. 2021. Allantoin: emerging role in plant abiotic stress tolerance. Plant Mol Biol Rep 39:648–661. https://doi.org/10.1007/s11105-021-01280-z
87. Kaur R, Chandra J, Varghese B, Keshavkant S. 2023. Allantoin: a potential compound for the mitigation of adverse effects of abiotic stresses in plants. Plants (Basel) 12:3059. https://doi.org/10.3390/plants12173059
88. Izaguirre-Mayoral ML, Lazarovits G, Baral B. 2018. Ureide metabolism in plant-associated bacteria: purine plant-bacteria interactive scenarios under nitrogen deficiency. Plant Soil 428:1–34. https://doi.org/10.1007/s11104-018-3674-x
89. Navone L, Casati P, Licona-Cassani C, Marcellin E, Nielsen LK, Rodriguez E, Gramajo H. 2014. Allantoin catabolism influences the production of antibiotics in *Streptomyces coelicolor*. Appl Microbiol Biotechnol 98:351–360. https://doi.org/10.1007/s00253-013-5372-1
90. Bayer B, Hansman RL, Bittner MJ, Noriega‐Ortega BE, Niggemann J, Dittmar T, Herndl GJ. 2019. Ammonia‐oxidizing archaea release a suite of organic compounds potentially fueling prokaryotic heterotrophy in the ocean. bioRxiv. https://doi.org/10.1101/558726
91. Kujawinski EB, Braakman R, Longnecker K, Becker JW, Chisholm SW, Dooley K, Kido Soule MC, Swarr GJ, Halloran K. 2023. Metabolite diversity among representatives of divergent *Prochlorococcus* ecotypes. mSystems 8:e0126122. https://doi.org/10.1128/msystems.01261-22
92. Mooshammer M, Wanek W, Jones SH, Richter A, Wagner M. 2021. Cyanate is a low abundance but actively cycled nitrogen compound in soil. Commun Earth Environ 2:1–10. https://doi.org/10.1038/s43247-021-00235-2
93. Widner B, Mulholland MR, Mopper K. 2016. Distribution, sources, and sinks of cyanate in the Coastal North Atlantic Ocean. Environ Sci Technol Lett 3:297–302. https://doi.org/10.1021/acs.estlett.6b00165
94. Zhu Y, Mulholland MR, Macías Tapia A, Echevarría MA, Pérez Vega E, Bernhardt P. 2023. Cyanate dynamics under algal blooms and sediment resuspension events in a shallow micro-tidal estuary in the lower Chesapeake Bay. Estuar Coast Shelf Sci 281:108188. https://doi.org/10.1016/j.ecss.2022.108188
95. Wang R, Liu J, Xu Y, Liu L, Mopper K. 2024. Unraveling sources of cyanate in the marine environment: insights from cyanate distributions and production during the photochemical degradation of dissolved organic matter. Front Mar Sci 11. https://doi.org/10.3389/fmars.2024.1373643
96. Purcarea C, Ahuja A, Lu T, Kovari L, Guy HI, Evans DR. 2003. *Aquifex aeolicus* aspartate transcarbamoylase, an enzyme specialized for the efficient utilization of unstable carbamoyl phosphate at elevated temperature. J Biol Chem 278:52924–52934. https://doi.org/10.1074/jbc.M309383200
97. Ter-Ovanessian LMP, Rigaud B, Mezzetti A, Lambert J-F, Maurel M-C. 2021. Carbamoyl phosphate and its substitutes for the uracil synthesis in origins of life scenarios. Sci Rep 11:19356. https://doi.org/10.1038/s41598-021-98747-6
98. Cheng G, Shapir N, Sadowsky MJ, Wackett LP. 2005. Allophanate hydrolase, not urease, functions in bacterial cyanuric acid metabolism. Appl Environ Microbiol 71:4437–4445. https://doi.org/10.1128/AEM.71.8.4437-4445.2005
99. USEPA. 2015. Nonpoint source: agriculture. Overviews and factsheets. Available from: https://www.epa.gov/nps/nonpoint-source-agriculture. Retrieved 24 Apr 2025.
100. Ding S, Li C, Ding X, Li G, Ban G, Xia Z, Zhao X, Lin Q, Wang X. 2022. An exploration of manure derived N in soils using ^{15}N after the application of biochar, straw and a mix of both. Sci Total Environ 804:150239. https://doi.org/10.1016/j.scitotenv.2021.150239
101. Das S, Jeong ST, Das S, Kim PJ. 2017. Composted cattle manure increases microbial activity and soil fertility more than composted swine manure in a submerged rice paddy. Front Microbiol 8:1702. https://doi.org/10.3389/fmicb.2017.01702
102. Beattie RE, Bandla A, Swarup S, Hristova KR. 2020. Freshwater sediment microbial communities are not resilient to disturbance from agricultural land runoff. Front Microbiol 11:539921. https://doi.org/10.3389/fmicb.2020.539921
103. Farrell M, Prendergast-Miller M, Jones DL, Hill PW, Condron LM. 2014. Soil microbial organic nitrogen uptake is regulated by carbon availability. Soil Biol Biochem 77:261–267. https://doi.org/10.1016/j.soilbio.2014.07.003
104. Marier JR, Rose D. 1964. Determination of cyanate, and a study of its accumulation in aqueous solutions of urea. Anal Biochem 7:304–314. https://doi.org/10.1016/0003-2697(64)90135-6
105. Dirnhuber P, Schütz F. 1948. The isomeric transformation of urea into ammonium cyanate in aqueous solutions. Biochem J 42:628–632. https://doi.org/10.1042/bj0420628
106. Vaishnav A, Kumar R, Singh HB, Sarma BK. 2022. Extending the benefits of PGPR to bioremediation of nitrile pollution in crop lands for enhancing crop productivity. Sci Total Environ 826:154170. https://doi.org/10.1016/j.scitotenv.2022.154170
107. Dwivedi D, Steefel CI, Arora B, Banfield J, Bargar J, Boyanov MI, Brooks SC, Chen X, Hubbard SS, Kaplan D, Kemner KM, Nico PS, O'Loughlin EJ, Pierce EM, Painter SL, Scheibe TD, Wainwright HM, Williams KH, Zavarin M. 2022. From legacy contamination to watershed systems science: a review of scientific insights and technologies developed through DOE-supported research in water and energy security. Environ Res Lett 17:043004. https://doi.org/10.1088/1748-9326/ac59a9
108. Freeman EC, Mudunuru MK, Feeser KL, McClure EA, González-Pinzón R, Ward CS, Bottos EM, Krause S, Peña J, Newcomer ME. 2025. Molecular diversity of dissolved organic matter reflects macroecological patterns in river networks. Sci Rep 15:27019. https://doi.org/10.1038/s41598-025-12835-5
109. Hendrickson TL. 2018. Old enzymes versus new herbicides. J Biol Chem 293:7892–7893. https://doi.org/10.1074/jbc.H118.002878
110. Boye K, Bobb C, Tolar B, Maher K, Francis C, Bargar J. 2020. Depth-resolved soil data from DOE-LM Riverton Wyoming site, April-September 2017
111. Uritskiy GV, DiRuggiero J, Taylor J. 2018. MetaWRAP—a flexible pipeline for genome-resolved metagenomic data analysis. Microbiome 6:158. https://doi.org/10.1186/s40168-018-0541-1
112. Kang DD, Li F, Kirton E, Thomas A, Egan R, An H, Wang Z. 2019. MetaBAT 2: an adaptive binning algorithm for robust and efficient genome reconstruction from metagenome assemblies. PeerJ 7:e7359. https://doi.org/10.7717/peerj.7359
113. Wu Y-W, Simmons BA, Singer SW. 2016. MaxBin 2.0: an automated binning algorithm to recover genomes from multiple metagenomic datasets. Bioinformatics 32:605–607. https://doi.org/10.1093/bioinformatics/btv638
114. Alneberg J, Bjarnason BS, Bruijn I, Schirmer M, Quick J, Ijaz UZ, Loman NJ, Andersson AF, Quince C. 2013. CONCOCT: clustering cONtigs on COverage and ComposiTion. arXiv. https://doi.org/10.48550/arXiv.1312.4038
115. Nayfach S, Shi ZJ, Seshadri R, Pollard KS, Kyrpides NC. 2019. New insights from uncultivated genomes of the global human gut microbiome. Nature 568:505–510. https://doi.org/10.1038/s41586-019-1058-x
116. Eren AM, Esen ÖC, Quince C, Vineis JH, Morrison HG, Sogin ML, Delmont TO. 2015. Anvi'o: an advanced analysis and visualization platform for 'omics data. PeerJ 3:e1319. https://doi.org/10.7717/peerj.1319
117. Parks DH, Imelfort M, Skennerton CT, Hugenholtz P, Tyson GW. 2015. CheckM: assessing the quality of microbial genomes recovered from isolates, single cells, and metagenomes. Genome Res 25:1043–1055. https://doi.org/10.1101/gr.186072.114
118. Olm MR, Brown CT, Brooks B, Banfield JF. 2017. dRep: a tool for fast and accurate genomic comparisons that enables improved genome recovery from metagenomes through de-replication. ISME J 11:2864–2868. https://doi.org/10.1038/ismej.2017.126
119. Chaumeil P-A, Mussig AJ, Hugenholtz P, Parks DH. 2020. GTDB-Tk: a toolkit to classify genomes with the Genome Taxonomy Database. Bioinformatics 36:1925–1927. https://doi.org/10.1093/bioinformatics/btz848
120. Langmead B, Salzberg SL. 2012. Fast gapped-read alignment with Bowtie 2. Nat Methods 9:357–359. https://doi.org/10.1038/nmeth.1923
121. Aroney STN, Newell RJP, Nissen JN, Camargo AP, Tyson GW, Woodcroft BJ. 2025. CoverM: Read alignment statistics for metagenomics. arXiv. https://doi.org/10.48550/arXiv.2501.11217
122. Kanehisa M, Goto S. 2000. KEGG: kyoto encyclopedia of genes and genomes. Nucleic Acids Res 28:27–30. https://doi.org/10.1093/nar/28.1.27
123. Kanehisa M, Furumichi M, Sato Y, Matsuura Y, Ishiguro-Watanabe M. 2025. KEGG: biological systems database as a model of the real world. Nucleic Acids Res 53:D672–D677. https://doi.org/10.1093/nar/gkae909

124. Kanehisa M, Sato Y, Morishima K. 2016. BlastKOALA and GhostKOALA: KEGG tools for functional characterization of genome and metagenome sequences. J Mol Biol 428:726–731. https://doi.org/10.1016/j.jmb.2015.11.006
125. Huerta-Cepas J, Szklarczyk D, Heller D, Hernández-Plaza A, Forslund SK, Cook H, Mende DR, Letunic I, Rattei T, Jensen LJ, von Mering C, Bork P. 2019. eggNOG 5.0: a hierarchical, functionally and phylogenetically annotated orthology resource based on 5090 organisms and 2502 viruses. Nucleic Acids Res 47:D309–D314. https://doi.org/10.1093/nar/gky1085
126. Cantalapiedra CP, Hernández-Plaza A, Letunic I, Bork P, Huerta-Cepas J. 2021. eggNOG-mapper v2: functional annotation, orthology assignments, and domain prediction at the metagenomic scale. Mol Biol Evol 38:5825–5829. https://doi.org/10.1093/molbev/msab293
127. Matheus Carnevali P, Hobson C, Geller-McGrath D, Dong W, Falco N, Wainwright H, Lavy A, Thomas A, Sharrar A, Lei S, WilliamsKH, Banfield J. 2020. *Genome-resolved metagenomics and metatranscriptomics of microbial communities in three meander-bound floodplain soils along the East River, Colorado*. Watershed Function SFA, ESS-DIVE repository.
128. Veltri D, Wight MM, Crouch JA. 2016. SimpleSynteny: a web-based tool for visualization of microsynteny across multiple species. Nucleic Acids Res 44:W41–W45. https://doi.org/10.1093/nar/gkw330
129. Sievers F, Wilm A, Dineen D, Gibson TJ, Karplus K, Li W, Lopez R, McWilliam H, Remmert M, Söding J, Thompson JD, Higgins DG. 2011. Fast, scalable generation of high‐quality protein multiple sequence alignments using Clustal Omega. Mol Syst Biol 7:539. https://doi.org/10.1038/msb.2011.75
130. Edgar RC. 2004. MUSCLE: multiple sequence alignment with high accuracy and high throughput. Nucleic Acids Res 32:1792–1797. https://doi.org/10.1093/nar/gkh340
131. Minh BQ, Schmidt HA, Chernomor O, Schrempf D, Woodhams MD, von Haeseler A, Lanfear R. 2020. IQ-TREE 2: new models and efficient methods for phylogenetic inference in the genomic era. Mol Biol Evol 37:1530–1534. https://doi.org/10.1093/molbev/msaa015
132. Kalyaanamoorthy S, Minh BQ, Wong TKF, von Haeseler A, Jermiin LS. 2017. ModelFinder: fast model selection for accurate phylogenetic estimates. Nat Methods 14:587–589. https://doi.org/10.1038/nmeth.4285
133. Rambaut A. 2010. FigTree. Available from: http://tree.bio.ed.ac.uk/software/figtree/. Retrieved 18 Jul 2024.
134. Letunic I, Bork P. 2024. Interactive Tree of Life (iTOL) v6: recent updates to the phylogenetic tree display and annotation tool. Nucleic Acids Res 52:W78–W82. https://doi.org/10.1093/nar/gkae268
135. Rasmussen A, Langenfeld K, Cardarelli E, Maher K, Bargar J, Boye K, Francis C. 2025. Metagenome-assembled genomes from Wind River Basin floodplain sediments Riverton, Wyoming site (August 2015). Groundwater Quality SFA, ESS-DIVE repository.
136. Rasmussen A, Langenfeld K, Tolar B, Bobb C, Maher K, Bargar J, Boye K, Francis C. 2025. Metagenome-assembled genomes from Wind River Basin floodplain sediments Riverton, Wyoming site (May to September 2017). ESS-DIVE. https://doi.org/10.15485/2563574
137. Rasmussen A, Langenfeld K, Perzan Z, Tolar B, Maher K, Bargar J, Boye K, Francis C. 2025. Metagenome-assembled genomes from Wind River Basin floodplain sediments Riverton, Wyoming site (June to October 2019). Groundwater Quality SFA, ESS-DIVE repository.